O conteúdo do presente relatório é de única responsabilidade do(s) autor(es).
The contents of this report are the sole responsibility of the author(s).

Exact Solutions of Rectangular Partitions via Integer Programming

Cláudio Nogueira de Meneses

Cid Carvalho de Souza

Relatório Técnico IC–98-35

Outubro de 1998

Exact Solutions of Rectangular Partitions via Integer Programming [†]

Cláudio Nogueira de Meneses [‡] *Cid Carvalho de Souza* [§]

Abstract

We are given a rectangle R in the plane and a finite set P of n points in the interior of R. A rectangular partition of R is a partition of the surface of R into smaller rectangles. A rectangular partition is said to be feasible with respect to P if no points in P lie in the strict interior of any rectangle of the partition. The length of a rectangular partition is computed as the sum of the lengths of the straight line segments that define the boundary of its rectangles. The goal is to find a (feasible) rectangular partition whose length is minimized. This problem, denoted here by RGP, is $\mathcal{NP}$-hard and has application in VLSI design. Several approximation algorithms have been proposed in the literature to solve it. In this paper we investigate how to obtain exact solutions for the RGP. We introduce two different Integer Programming formulations. To test these formulations computationally we have implemented a Branch-and-Cut algorithm and a Branch-and-Price algorithm for the first and the second formulation, respectively. Comparisons between the two formulations are made. The computational results with a randomly generated set of instances show that it is possible to solve exactly medium-sized instances of the RGP. Moreover, we show that the size of the instances that can be solved with our algorithms decrease by an order of magnitude in the absence of corectilinear points in P, a special case of RGP whose complexity is still open. Finally we also have implemented the best approximation algorithm known for RGP and we show that it usually produces solutions about 10% off the optimum.

Keywords: Rectangular Partition, Polyhedral Combinatorics, Branch-and-Cut, Branch-and-Price.

1 Introduction

In this paper we study the following problem. Given a rectangle R in the plane and a finite set P of n points in the interior of R, a *rectangular partition* of R is a partition of the surface of R into smaller rectangles. A rectangular partition is said to be *feasible with respect to*

[†]This research was supported by FAPESP (grant number 96/0945-8) and by CNPq (grant number 300883/94-3)

[‡]Universidade Estadual de Campinas, Instituto de Computação, Campinas/SP, Brazil (*e-mail: nogueira@dcc.unicamp.br*)

[§]corresponding author: Universidade Estadual de Campinas, Instituto de Computação, C.P. 6176, 13083-970, Campinas/SP,Brazil (*e-mail: cid@dcc.unicamp.br*)

P, if no points in P lie in the strict interior of any rectangle of the partition. The *length* of a rectangular partition is computed as the sum of the lengths of the straight line segments that define the boundary of its rectangles. The goal is to find a feasible rectangular partition whose length is minimum.

In the remaining of the text, we denote this problem by RGP. For sake of brevity, unless when specified otherwise, the term *partition* is used here to refer to a *feasible rectangular partition*.

The RGP belongs to large class of problems involving the optimal partitioning of rectilinear polygons with holes inside. A hole can be either a rectilinear polygon or a point, and the objective function may vary. As we will see later in Section 2 most of these problems belong to the class $\mathcal{NP}$-hard.

These problems have brought to the attention of researchers in Computational Geometry mainly due to their practical application in VLSI design ([11]). The surface of the external rectangle R models the surface of the circuit and the points in P the terminals in the nets to be routed. The segments inducing a partition of R define the *channels* in which routing has to be done. By minimizing the length of the partition we aim to minimize the overall length of the routing.

Several approximation algorithms have been proposed in the literature for the RGP (see next Section). However, to the best of our knowledge, no exact algorithm has been tried to tackle the problem. In this paper we study different Integer Programming (IP) formulations for the RGP. After having formulated the problem, we use IP techniques such as Branch-and-Cut and Branch-and-Price algorithms to search for optimal solutions. We have implemented these algorithms and we report the computational results obtained on a set of randomly generated medium-sized instances. The results are quite promising and suggest that IP can be used to solve further variants of rectangular partition problems exactly.

We compare both theoretically and in practice the two alternative IP models and we also evaluate the performance of the best known approximation algorithm for the RGP.

The paper is organized as follows. The next Section gives a brief overview of previous works on complexity analysis and approximation algorithms for the RGP. Section 3 contains some basic definitions and introduces two important theorems which ensure the validity of the IP models presented later. In Section 4 we discuss our first IP formulation for the RGP and, using Polyhedral Combinatorics techniques, we show how to tighten this formulation. In Section 5 we reformulate the problem using new variables, which leads to a special case of the classical set partitioning problem. We compare the two alternative models not only in terms of number of constraints and variables but, specially in terms of the bounds provided by their linear relaxations. Section 6 describes some details of the Branch-and-Cut and Branch-and-Price algorithms we have implemented for the formulations given in Sections 4 and 5 respectively. In this Section we also report and discuss our computational results. Finally, in Section 7, we draw some conclusions and discuss some future directions for research in this topic.

2 Previous Work: short overview

In this Section, we characterize the RGP as a particular case of a class of polygons partition problems. The computational complexities of these problems are presented and finally we shortly discuss the main approximation algorithms proposed for the RGP.

In a general rectangular partition problem R is a rectilinear polygon, that is, a polygon whose sides are parallel to the axes, which is not necessarily a rectangle. Moreover, P is a finite set of n non-intersecting holes in the surface of R, where a *hole* is either a point or another rectilinear polygon. The goal is to partition the surface of R into smaller rectangles with no holes of P in the interior, such that the sum of the lengths of all straight lines that induce the partition is minimized (other objective functions such as minimizing the number of rectangles in the partition are not considered here).

Special cases of this problem are derived by limiting R to be a rectangle and/or restricting the holes to be points. The complexities of these variants of the original problem have been investigated since the early 80's. They are summarized in Table 1 below which is taken from [5]. The problems are characterized according to the shape of R and the type of holes.

Problem	External Boundary	Holes	Complexity
RPHF	Rectilinear Polygon	Hole Free	$\mathcal{P}$
RGNLP	Rectangle	Noncorectilinear Points	$\mathcal{NP}$
RPNLP	Rectilinear Polygon	Noncorectilinear Points	$\mathcal{NP}$
RGP	Rectangle	Points	$\mathcal{NP}$-hard
RPP	Rectilinear Polygon	Points	$\mathcal{NP}$-hard
RGRP	Rectangle	Rectilinear Polygons	$\mathcal{NP}$-hard
RPRP	Rectilinear Polygon	Rectilinear Polygons	$\mathcal{NP}$-hard
RGRPP	Rectangle	Rectilinear Polygons and Points	$\mathcal{NP}$-hard
RPRPP	Rectilinear Polygon	Rectilinear Polygons and Points	$\mathcal{NP}$-hard

Table 1: Complexities of Rectangular Partition Problems.

From Table 1, one can note that in the absence of holes the problem is easy ([11]). Excepting for rows 2 and 3, all other cases have been proved to be in $\mathcal{NP}$-hard. Rows 2 and 3 refer to the case where all holes are given by points and no two of these belong to the same horizontal or vertical line. When this holds, the set of holes P is said to be *noncorectilinear*. In this case, the complexity of the problem remains open. We are going to show later in Section 6, that those are by far the most difficult instances to solve with our approach.

Figure 1 is also taken from [5]. It shows polynomial reductions between the problems of Table 1. The notation $A \rightarrow B$ is used to denote that problem A reduces polynomially to problem B.

From now on, we focus on the RGP problem but, as suggested by the reduction depicted

in Figure 1, RGNLP is a special case of RGP and, therefore, our study immediately extends to that case.

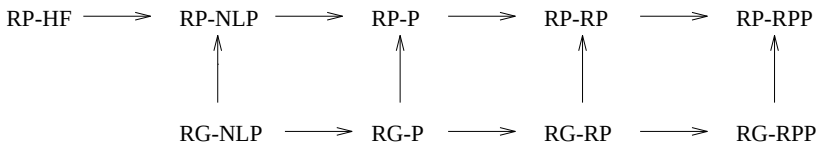

Figure 1: Polynomial Reductions between Rectangular Partition Problems

Most of the research that has been done on the RGP is concentrated in the development of approximation algorithms. In [5], Gonzalez and Zheng have designed an $O(n^2)$ algorithm using a divide-and-conquer strategy whose worst case performance ratio is given by $3 + \sqrt{3}$. In [10], Levcopoulos has shown that this algorithm could actually be implemented in $O(n \log n)$.

Gonzalez and Zheng introduce another approximation algorithm in [7]. The worst case performance ratio of this algorithm decrease to 3 relative to their first algorithm, but its complexity increased to $O(n^4)$. This algorithm has two basic steps. In the first one the problem is transformed in an instance of the RPFH (see Table 1). In the second step the RPHF problem is solved by an $O(n^4)$ dynamic programming algorithm proposed in [11].

The best approximation algorithm for the RGP has worst case performance ratio of 1.75. It has been proposed by Du, Pand and Shing ([2]) and it also uses dynamic programming. These authors proved that the performance ratio of the algorithm is at most 2. An easier proof of that fact is given in [3]. However, a better bound for the performance of the algorithm was achieved by Gonzalez and Zheng in [6] who proved that the length of the partition produced by the algorithm is at most 1.75 larger than the length of an optimal solution.

The algorithm proposed by Du, Pand and Shing finds an optimal *guillotine* partition of R. A guillotine partition is a partition induced by a set of straight line segments with the following property. If we broke the rectangle R recursively following these straight lines, at each iteration in this process, either there exists a straight line dividing the current rectangle into two smaller ones or the current rectangle belongs to the partition and has no straight line in its interior. Figure 2 shows an instance of the RGP and two partitions. The partition in (b) is not guillotine and the one in (c) is a guillotine partition.

Clearly, the optimal solution for an instance of the RGP is not necessarily a guillotine partition. Actually, in our computational experiments it never happened that Du, Pand and Shing algorithm solve the RGP exactly.

Table 2 summarizes the best known approximation algorithms for the RGP. We have not been able to find in the literature exact algorithms to solve the problem. Our goal is to develop such an algorithm using Integer Programming techniques. Thus, in the next Section we introduce some results that are fundamental to validate our formulations.

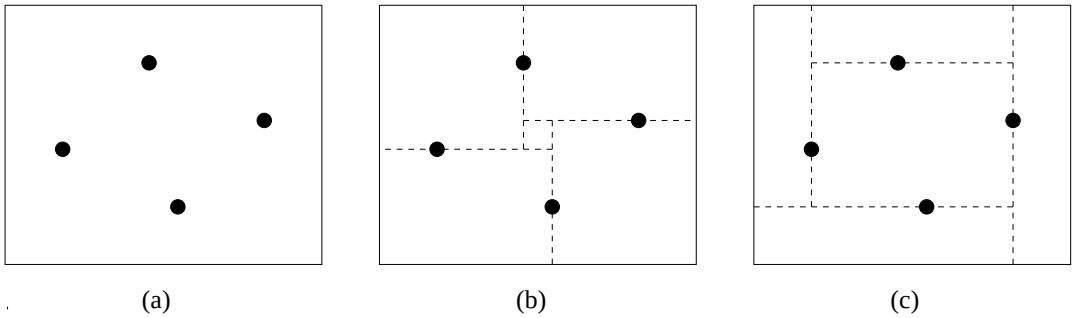

Figure 2: (a) Instance of the RGP (b) Nonguillotine partition (c) Guillotine partition.

Worst Case Performance Ratio	Complexity	Reference	Strategy
$3+\sqrt{3}$	$O(n^2)$,$O(n \log n)$	[5, 10]	Divide and Conquer
4	$O(n \log n)$	[4]	Divide and Conquer
3	$O(n^4)$	[7]	Dynamic Programming
2	$O(n^5)$	[2, 3]	Dynamic Programming
1.75	$O(n^5)$	[6]	Dynamic Programming

Table 2: Best approximation algorithms for the RGP.

3 Definitions and Fundamental Results

An important result about the optimal solutions of the RGP due to Lingas *et al.* ([11]) is given in Theorem 3.1. According to this result, the straight line segments inducing any optimal partition for an instance of the RGP lie on a finite set of horizontal and vertical lines. This property allows us to look at the RGP as a discrete optimization problem.

Before stating the theorem, we have to introduce some definitions.

Definition 3.1 *Let $I = (R, P)$ be an instance of the RGP. The* **grid** *induced by P, denoted by* GI(P)*, is the set of straight line segments defined in the interior of R by the vertical and horizontal lines intersecting the points in P.*

A point p is a *grid point* if it belongs to the interior of R and it is in the intersection of a horizontal and a vertical line containing segments of GI(P). These points are partitioned into two sets. The set of **terminal** points, which are those points in P, and the set of **Steiner** points which are not in P. Figure 3 illustrate these definitions. Dotted circles represent the terminal points while empty circles represent the Steiner points.

In the remaining of the text, we shall use the term *grid segment* to denote a segment containing precisely two grid points which are located at its extremities. Thus, in Figure 3 we have 24 grid segments.

We now give the fundamental theorem of Lingas *et al.* .

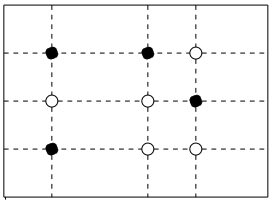

Figure 3: An instance $I = (R, P)$ of the RGP with 4 terminals and 5 Steiner points. The dotted segments are those in the grid GI(P).

Theorem 3.1 *[11] In any optimal solution S^* of an instance $I = (R, P)$ of the RGP, all straight line segments inducing the partition lie on the grid GI(P).*

A natural consequence of this theorem is that the RGP can be viewed as a problem of deciding whether or not each of the grid segments is in an optimal solution. This is the first step to formulate the problem as a 0-1 Integer Programming problem. However, this is not enough since clearly not all subsets of grid segments induce a rectangular partition.

There are two geometric configurations that are forbidden for a set of grid segments to form a rectangular partition of R. These configurations are defined below.

Definition 3.2 *Let $I = (R, P)$ be an instance of the RGP. A subset C of grid segments in GI(P) is said to define a* **knee** *in a grid point q (terminal or Steiner) if there are exactly two grid segments of C incident in q and these segments are orthogonal. Moreover, C is said to define an* **island** *in a grid point q (terminal or Steiner) if there is exactly one grid segment of C incident in q.*

The knee and island configurations are depicted in Figure 4.

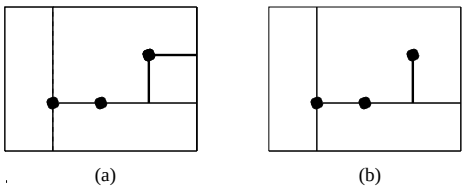

Figure 4: (a) A knee and (b) an island configuration at a terminal point.

The next theorem establish the necessary conditions for a subset of grid segments to form a feasible rectangular partition of R with respect to P.

Theorem 3.2 *Given an instance $I = (R, P)$ of the RGP, let C be a subset of grid segments in GI(P) not containing knees and islands and such that every terminal point in P has at least two segments of C incident to it. Then, C induces a feasible rectangular partition of R with respect to P.*

Proof: The segments in C together with those at the boundary of R induce a partition of the plane such that, as C has no islands (vertices of degree one), each face in the partition is a polygon which may be not simply connected (i.e., with holes).

Assume that there exists a face F of the partition induced by C which is a polygon with at least one hole H. The (external) border of H is, by definition, not connected to the border of F, and therefore, its upper and rightmost vertex has degree 2 (is a knee). This is a contradiction.

Thus, all the faces are simply connected polygons. Since the only convex polygons, with vertices and sides restricted to GI(P), are rectangles, it is enough to show that all the faces are convex.

Suppose, in the contrary, that there is a non convex face. Since this face is simply connected, it must have a vertex with a reflex internal angle. The restriction on segments of GI(P), implies that the only possibilities for reflex angles are 270 or 360 degrees respectively, knees or islands. Again this is a contradiction, which completes the proof. □

Theorems 3.1 and 3.2 allow us to formulate the RGP in terms of an Integer Programming (IP) problem. This is done in the next two sections.

4 An Integer Programming formulation for RGP: the segment model

To be able to use IP techniques to solve RGP instances exactly we have to find a valid IP formulation for the problem. This Section presents our first IP formulation for the RGP and it is organized as follows. In the next subsection we describe the original formulation and show its validity. In the second subsection, we study the polytope associated to the convex hull of feasible solutions of this formulation. We introduce several classes of facet defining inequalities that can be used to tighten the original formulation and, therefore, are candidates to be used in a cutting plane algorithm for solving the RGP.

4.1 The Original Formulation

From Theorem 3.1, it is natural to formulate the problem using binary decision variables associated to each of the grid segments. These variables assume the value 1 or 0 depending whether or not they belong to the straight lines defining the partition. Reasoning in this way, the vector of variables can be seen as the characteristic vector of a subset of grid segments. However, we have to restrict ourselves to the feasible subsets of grid segments, i.e., to the subsets that induce rectangular partitions of R with respect to P. Those subsets are characterized in Theorem 3.2 and what remains to be done is to describe these restrictions in terms of set of linear inequalities. Let us formalize these ideas.

Initially, for each grid segment $e \in$ GI(P), we define the variable x_e such that:

$$x_e = \begin{cases} 1 & \text{if the grid segment } e \text{ belongs to a solution } S, \\ 0 & \text{otherwise.} \end{cases}$$

Let m be the number of grid segments in GI(P). The vector $x \in \mathbb{R}^m$ whose components are defined above is the characteristic or incidence vector of a feasible rectangular partition S. According to this notation, if $d \in \mathbb{R}^m$ is the vector defined such that the e-th component

of d is the length of segment e of GI(P), then the objective function of the RGP is to find the minimum of $dx = \sum_{e=1}^{m} d_e x_e$.

Now, to describe the constraints we introduce the following convention. For each grid point i (either a terminal or a Steiner), the indexes $i_{(1)}, i_{(2)}, i_{(3)}$ e $i_{(4)}$ refer to the segments incident in i as indicated in Figure 5. Using this notation, the RGP can be formulated as:

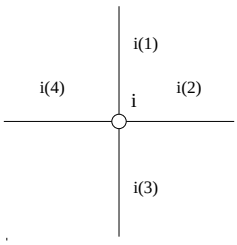

Figure 5: Grid segments incident to a point i.

$$\text{Minimize} \sum_{e=1}^{m} d_e x_e$$

Subject to

$$\left.\begin{array}{ll} x_{i(1)} + x_{i(2)} \geq 1 & (1) \\ x_{i(1)} + x_{i(4)} \geq 1 & (2) \\ x_{i(3)} + x_{i(2)} \geq 1 & (3) \\ x_{i(3)} + x_{i(4)} \geq 1 & (4) \end{array}\right\} \quad \text{for each terminal point } i \text{ in GI}(P)$$

$$\left.\begin{array}{ll} x_{i(1)} + x_{i(2)} - x_{i(3)} \geq 0 & (5) \\ x_{i(1)} + x_{i(2)} - x_{i(4)} \geq 0 & (6) \\ x_{i(1)} + x_{i(4)} - x_{i(2)} \geq 0 & (7) \\ x_{i(1)} + x_{i(4)} - x_{i(3)} \geq 0 & (8) \\ x_{i(3)} + x_{i(2)} - x_{i(1)} \geq 0 & (9) \\ x_{i(3)} + x_{i(2)} - x_{i(4)} \geq 0 & (10) \\ x_{i(3)} + x_{i(4)} - x_{i(1)} \geq 0 & (11) \\ x_{i(3)} + x_{i(4)} - x_{i(2)} \geq 0 & (12) \end{array}\right\} \quad \text{for each Steiner point } i \text{ in GI}(P)$$

$$\begin{array}{ll} 0 \leq x \leq 1 & (13) \\ x \ \textit{integer} & (14) \end{array}$$

We call inequalities (1) to (4) the *Class I* inequalities while those from (5) to (12) are called *Class II* inequalities. The previous formulation has $O(n^2)$ variables, $O(n)$ Class I constraints and $O(n^2)$ Class II constraints. We now establish the results ensuring the validity of the formulation.

Proposition 4.1 *Class I inequalities avoid the knee and island configurations at terminal points.*

Proof: Assume that x is the incidence vector of an arbitrary feasible partition.

To prove the proposition it is enough to analyze the following cases. Consider the instance of the RGP depicted in Figure 6. To show that Class I inequalities avoid the existence of an island, assume that $x_{i(1)} = 1$ and $x_{i(2)} = x_{i(3)} = x_{i(4)} = 0$, which implies the existence of an island at the terminal point i. In this case, inequalities (3) and (4) are violated. Similar arguments show that the other three possibilities of islands at point i violate at least one of the inequalities in Class I.

Now, to show that Class I inequalities avoid the existence of a knee at the terminal point i, assume that $x_{i(2)} = x_{i(3)} = 1$ and $x_{i(1)} = x_{i(4)} = 0$. In this case, inequality (2) is violated. Symmetric arguments show that the other three knees at point i violate one of the inequalities in Class I. □

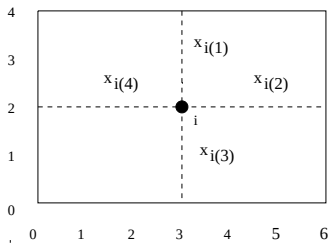

Figure 6: Instance of the RGP for the proof of Proposition 4.1.

Proposition 4.2 *Class II inequalities avoid the knee and island configurations at Steiner points.*

Proof: Assume that x is the incidence vector of an arbitrary feasible partition.

Consider the instance shown in Figure 7. Initially let us suppose that $x_{i(1)} = 1$ and $x_{i(2)} = x_{i(3)} = x_{i(4)} = 0$ which defines an island at the Steiner point i. In this case, both inequalities (9) and (11) of Class II are violated. Moreover, if $x_{i(1)} = x_{i(2)} = 1$ and $x_{i(3)} = x_{i(4)} = 0$, there is a knee defined at the Steiner point i. In this case, inequalities (11) and (12) of Class II are violated. By symmetric arguments, we conclude that all knees and islands at point i are eliminated by Class II inequalities. □

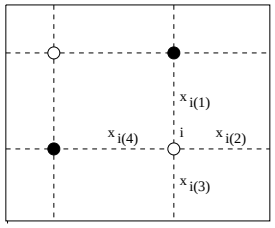

Figure 7: Instance of the RGP for the proof of Proposition 4.2.

The results in Propositions 4.1 and 4.2 allow us to establish the correctness of the IP formulation above.

Theorem 4.1 *A vector $x^S \in \mathbb{R}^m$ is the incidence vector of a feasible rectangular partition S if and only if x^S satisfies the constraints (1) to (14).*

Proof: We have to show that $x^S \in \mathbb{R}^m$ satisfies constraints (1) to (14) if and only if S is a rectangular partition of R with respect to P, where x^S is the incidence vector of S.

The necessity part goes as follows. First note that inequalities (1) and (4) of Class I indicate that S has at least two grid segments incident to each terminal point. Moreover, since x^S satisfy all Class I and Class II inequalities, Propositions 4.1 and 4.2 ensure that S does not contain knees nor islands. Therefore, from Theorem 3.2, S is a rectangular partition of R with respect to P.

For sufficiency, it is enough to note that if S is a rectangular partition of R with respect to P, then S does not contain knees nor islands. Moreover, S has at least two segments incident to each terminal point. Thus, the incidence vector of S, x^S, clearly satisfies all the constraints from (1) to (14). □

We now investigate the strength of the formulation given by (1) to (14). To do so, in the next subsection, we study the facial structure of the polyhedron represented by the convex hull of all incidence vectors of feasible rectangular partitions of an instance of the RGP.

4.2 Strength of the Segment Model: a Polyhedral Study

IP algorithms are based on the solution of linear programs. The efficiency of these algorithms depend on the bounds provided by the linear relaxation of the formulation at hand, i.e. the linear program which is obtained by removing the integrality constraints from the original formulation.

Ideally, any IP problem can be solved by Linear Programming if the complete linear system describing the convex hull of the integer solutions is available. In practice, for $\mathcal{NP}$-hard problems, this complete system is usually unknown and it is unlike to be useful for algorithmic purposes since it is typically very large. However, many hard combinatorial optimization problems have been successfully solved using a partial description of the convex hull of integer solutions (cf. references in [12]). The success of this approach is closely related to our ability in obtaining facet defining inequalities for the convex hull of feasible solutions. Such inequalities, when used in the framework of a cutting plane or branch-and-cut algorithm, tend to improve the bound provided by the linear relaxation, reducing the time needed to solve the problem.

The facial structure of the convex hull of incidence vectors of integer solutions of a given IP problem is studied via polyhedral combinatorics techniques. We refer to [12] for an introduction to polyhedral combinatorics. In this work we limit ourselves to give very few definitions and results which are necessary for the understanding of the text.

In this section we investigate the strength of the formulation introduced in the previous subsection. For this, we state the conditions under which the inequalities in this linear system define facets of the convex hull of incidence vectors of feasible rectangular partitions. Then we go further by introducing other classes of facet defining inequalities that could also be added to the formulation in order to make it stronger. Below we summarize some definitions and results of Polyhedral Theory.

Basic Definitions and Results

A polyhedron $\mathcal{P}= \{x \in \mathbb{R}^m \ : \ Ax \leq b\}$ is called a *polytope* if $-\omega \leq x \leq \omega$ for all x in $\mathcal{P}$ for some constant vector $\omega \in \mathbb{R}^m_+$. The dimension of a polyhedron $\mathcal{P}$ denoted by $\dim(\mathcal{P})$, is the cardinality of any maximal affinelly independent subset of $\mathcal{P}$. We say that $\mathcal{P}$ is *full dimensional* if $\dim(\mathcal{P}) = m$, that is, $\mathcal{P}$ has the dimension of $\mathbb{R}^m$. A *valid inequality* for $\mathcal{P}$ is an inequality that is satisfied by all points in $\mathcal{P}$. If $\omega x \leq \omega_0$ is a valid inequality for $\mathcal{P}$, the *face* $\mathcal{F}_{(\omega,\omega_0)}$ defined by this inequality in $\mathcal{P}$ is given by $\mathcal{F}_{(\omega,\omega_0)} = \{x \in \mathcal{P} \ : \ \omega x = \omega_0\}$. Each face $\mathcal{F}_{(\omega,\omega_0)}$ is a polyhedron and if $\dim(\mathcal{F}_{(\omega,\omega_0)}) = \dim(\mathcal{P}) - 1$, we say that $\mathcal{F}_{(\omega,\omega_0)}$ is a *facet* of $\mathcal{P}$.

The main steps we use when proving that a valid inequality $\omega x \leq \omega_0$ defines a facet of a full dimensional polyhedron $\mathcal{P}$ can be summarized as follows. First, we have to show that the face $\mathcal{F}_{(\omega,\omega_0)}$ (defined as above) is such that $\mathcal{F}_{(\omega,\omega_0)} \cap \mathcal{P} \neq \emptyset$ (i.e., there exists a point in $\mathcal{P}$ which is not in $\mathcal{F}_{(\omega,\omega_0)}$). Then, we suppose that there exists a (generic) valid inequality $\pi x \leq \pi_0$ for $\mathcal{P}$ which defines the face $\mathcal{F}_{(\pi,\pi_0)} \supseteq \mathcal{F}_{(\omega,\omega_0)}$. Finally, to prove that $\omega x \leq \omega_0$ defines a facet of $\mathcal{P}$ we have to show that there exists $\alpha \in \mathbb{R}_+$ such that $\pi = \alpha\omega$ and $\pi_0 = \alpha\omega_0$. This is a well-known technique in Polyhedral Combinatorics called the indirect method.

The Polytope for the RGP

We denote by $\mathcal{P}_\mathcal{R}$ the polytope given by the convex hull of the integer solutions of the formulation given in subsection 4.1. Thus, from Theorem 4.1, we have that:

$$\mathcal{P}_\mathcal{R} = \text{conv}\{x^S \in \mathbb{R}^m \ : \ S \text{ is a rectangular partition of } R \text{ with respect to } P\},$$

where m is the number of grid segments in $\text{GI}(P)$.

To study the facets of $\mathcal{P}_\mathcal{R}$ we first have to find the dimension of this polytope. This is given in the next theorem.

Theorem 4.2 *The polytope $\mathcal{P}_\mathcal{R}$ is full-dimensional, i.e.,* $\dim(\mathcal{P}_\mathcal{R}) = m$.

Proof: Since $\mathcal{P}_\mathcal{R} \subset \mathbb{R}^m$, $\dim(\mathcal{P}_\mathcal{R}) \leq m$ and any subset of affinelly independent points in $\mathcal{P}_\mathcal{R}$ has at most $m+1$ elements. Thus, if we find a subset with exactly $m+1$ elements, the proof is complete. Notice that the vector $\mathbb{1}_m$ with all components equal to one is in $\mathcal{P}_\mathcal{R}$ since the set of all grid segments is a feasible rectangular partition. Moreover, if we remove exactly one grid segment, say i, from this solution, we still have a feasible rectangular partition whose incidence vector is given by $\mathbb{1}_m - v^i$, where v^i is the vector with all components equal to zero except component i which has value one. The set whose elements are all possible $\mathbb{1}_m - v^i$ vectors and the vector $\mathbb{1}_m$ has size $m+1$ and can easily be shown to be affinelly independent. □

We now give a partial characterization of the facial structure of $\mathcal{P}_\mathcal{R}$ by exhibiting some of its facet defining inequalities. The proof of facetness can be long and tedious. For this reason some of these proofs are given in the Appendix. However, we kept the short proofs to illustrate the techniques which we found to be interesting for further polyhedron

investigations on $\mathcal{P}_\mathcal{R}$. To make the proofs easier we introduce one additional definition and a lemma.

Definition 4.1 *The* support *of a valid inequality* $\sum_{e=1}^{m} \omega_e x_e \leq \omega_0$ *for* $\mathcal{P}_\mathcal{R}$ *is the set of grid segments* $e \in GI(P)$ *such that* $\omega_e \neq 0$. *The* support rectangle *of the inequality is the smallest rectangle containing the support of the inequality whose sides are parallel to those of the rectangle* R.

These definitions are illustrated in Figure 8 for a Class I inequality.

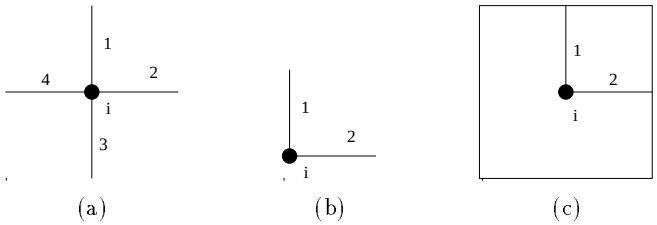

Figure 8: (a) Grid segments incident to a terminal point i. (b) Support of the inequality $x_1 + x_2 \geq 1$. (c) Support rectangle of the inequality $x_1 + x_2 \geq 1$.

Below, when proving that a given inequality defines a facet of $\mathcal{P}_\mathcal{R}$, we consider only the grid segments which are in the interior of the support rectangle of the inequality. This is justified by the following lemma.

Lemma 4.1 *Let* $\omega x \leq \omega_0$ *be a valid inequality for* $\mathcal{P}_\mathcal{R}$ *and* R_ω *its support rectangle. Moreover, let* $\mathcal{F}_{(\omega,\omega_0)}$ *be the face defined by* $\omega x \geq \omega_0$ *in* $\mathcal{P}_\mathcal{R}$. *If* $\pi x \leq \pi_0$ *is a valid inequality for* $\mathcal{P}_\mathcal{R}$ *defining the face* $\mathcal{F}_{(\pi,\pi_0)}$ *where* $\mathcal{F}_{(\pi,\pi_0)} \subseteq \mathcal{F}_{(\omega,\omega_0)}$, *then* $\pi_e = 0$ *for any grid segment* e *which is external to* R_ω.

Proof: Let $\mathcal{I}$ be an instance of the RGP, x the incidence vector of a feasible rectangular partition of $\mathcal{I}$ in the face $\mathcal{F}_{(\omega,\omega_0)}$ and $\overline{x}$ the incidence vector of another feasible rectangular partition of $\mathcal{I}$ obtained from x by adding all grid segments in the boundary and in the exterior of R_ω. For each grid segment e external to R_ω, define $\overline{x}^e$ as the vector obtained from $\overline{x}$ by setting the e-th component to zero. Clearly, $\overline{x}^e$ is the incidence vector of a feasible partition. Moreover, $\overline{x}$ and $\overline{x}^e$ lie on $\mathcal{F}_{(\omega,\omega_0)}$ and, by hypothesis, also on $\mathcal{F}_{(\pi,\pi_0)}$. Thus, we have that: $\pi\overline{x} = \pi\overline{x}^e = \pi_0$ which implies that $\pi_e = 0$. This completes the proof. □

In Theorems 4.3 and 4.4 below we investigate the facetness property relative to the trivial inequalities ($0 \leq x_e \leq 1$).

Theorem 4.3 *For all grid segment* s *in* $GI(P)$ *the inequality* $x_e \leq 1$ *defines a facet of* $\mathcal{P}_\mathcal{R}$.

Proof: The validity of the inequality is obvious. It is easy to see that the face $\mathcal{F}$ defined in $\mathcal{P}_\mathcal{R}$ by this inequality is such that $\mathcal{P}_\mathcal{R} \setminus \mathcal{F} \neq \emptyset$, since the incidence vector of the feasible partition formed by all grid segments but e does not lie on $\mathcal{F}$. This implies that $\dim(\mathcal{F}) \leq$

$\dim(\mathcal{P}_\mathcal{R}) - 1$. Now, using the same notation as in the proof of Theorem 4.2, consider the feasible solutions represented by the binary vectors $\mathbb{1}_m$ and $\mathbb{1}_m - v^j$ for all grid segments $j \neq e$. All these points are affinelly independent and lie on $\mathcal{F}$. Therefore, $\dim(\mathcal{F})$ is $m-1$ and the proof is complete. □

Theorem 4.4 *For all grid segment e in GI(P) the inequality $x_e \leq 0$ does not define a facet of $\mathcal{P}_\mathcal{R}$.*

Proof: We can show that a valid inequality does not define a facet of a full-dimensional polyhedron in two ways. First, we can show that it is a linear combination of two other valid inequalities. Alternatively, we can show that the face defined by this inequality is contained in the face defined by another inequality which is linearly independent from the original one.

Thus, assume initially that s is incident to a terminal point i. Moreover, w.l.o.g, let t be the next grid segment visited after e when the set of incident grid segments in i are traversed clockwise. If we sum up the Class I inequality $x_e + x_t \geq 1$ and $-x_t \geq -1$ we get the inequality $x_e \geq 0$. We conclude that this inequality is not facet defining for $\mathcal{P}_\mathcal{R}$.

Assume now that segment e is incident to a Steiner point i. Again, w.l.o.g, let t, u and v be the sequence in which the remaining grid segment incident to i are traversed if we proceed clockwise. Since i is a Steiner point, if $x_e = 0$, x_t and x_u are both zero or both one, since otherwise there will be either an island or a knee configuration with vertex in i. This implies that the face $\mathcal{F} = \{x \in \mathcal{P}_\mathcal{R} \ : \ x_e = 0\}$ is contained in the face $\{x \in \mathcal{P}_\mathcal{R} \ : \ x_e + x_t - x_v = 0\}$. Thus, $\mathcal{F}$ is not a facet of $\mathcal{P}_\mathcal{R}$. □

The next two Theorems consider inequalities in Class I and Class II.

Theorem 4.5 *Class I inequalities define facets of $\mathcal{P}_\mathcal{R}$.*

Proof: Validity of these inequalities have been shown in Theorem 4.1. If we denote by $\mathcal{F}_{(\omega,\omega_0)}$ the face defined by an arbitrary Class I inequality $\omega x \geq \omega_0$ in $\mathcal{P}_\mathcal{R}$, it is clear that $\mathcal{F}_{(\omega,\omega_0)} \neq \mathcal{P}_\mathcal{R}$ since the vector $\mathbb{1}_m \in \mathcal{P}_\mathcal{R} - \mathcal{F}_{(\omega,\omega_0)}$.

Let i be a terminal point and, for simplicity, let the grid segments incident to i be denoted by 1, 2, 3 and 4. Assume that these segments are arranged in the same order as segments $i_{(1)}, i_{(2)}, i_{(3)}$ and $i_{(4)}$ in Figure 5. We are going to show, w.l.o.g., that the Class I inequality $x_1 + x_2 \geq 1$ defines a facet of $\mathcal{P}_\mathcal{R}$. We use the standard technique to make the remaining of the proof.

Initially, we assume the existence of a valid inequality $\pi x \geq \pi_0$ which defines the face $\mathcal{F}_{(\pi,\pi_0)}$ in $\mathcal{P}_\mathcal{R}$. Moreover, we suppose that the face $\mathcal{F}_{(\omega,\omega_0)} = \{x \in \mathcal{P}_\mathcal{R} \ : \ x_1 + x_2 = 1\}$ is contained in $\mathcal{F}_{(\pi,\pi_0)}$. Using these facts, we show that the coefficients of vector π and π_0 are related in such a way that $\pi = \alpha\omega$ and $\pi_0 = \alpha\omega_0$ for some $\alpha \in \mathbb{R}_+$.

By Lemma 4.1, we know that $\pi_i = 0$ for any grid segment i external to the support rectangle of $x_1 + x_2 \geq 1$. We now have to consider the components of π corresponding to the remaining grid segments.

Case 1: Consider the two solutions illustrated in Figure 9. Note that x and $\overline{x}$ are in $\mathcal{F}_{(\omega,\omega_0)}$ and, by hypothesis, also in $\mathcal{F}_{(\pi,\pi_0)}$. Then, $\pi x = \pi\overline{x} = \pi_0$ which implies that $\pi_4 = 0$. Analogous arguments can be easily applied to prove that $\pi_3 = 0$.

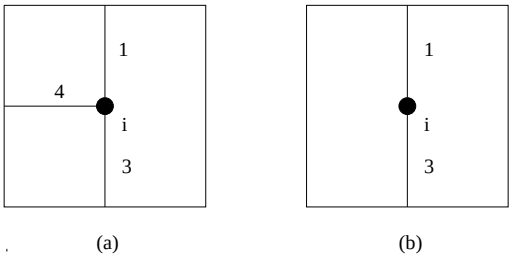

Figure 9: A terminal point i. In (a) is represented a solution whose incidence vector is $x = (x_1, \ldots, x_m) = (1, 0, 1, 1, \ldots, 1)$. In (b) is represented another solution with incidence vector given by $\overline{x} = (1, 0, 1, 0, 1, 1, \ldots, 1)$.

Case 2: Consider the solution shown in Figure 10. According to the symmetry, the results proved for segment A also hold for segment A'. This equivalence also applies to the pair of segments (B, B'), (C, C') and (D, D').

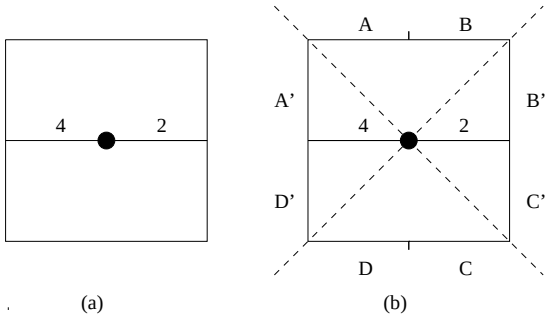

Figure 10: The incidence vector of the solution in (a) is given by $x = (0, 1, 0, 1, 1, \ldots, 1)$. In (b) the axis of symmetry for the support of the inequality $x_1 + x_2 \geq 1$ are represented.

If we remove A' (B', C', D') from the solution represented by x we obtain a new feasible solution whose incidence vector $x^{A'}$ ($x^{B'}$,$x^{C'}$,$x^{D'}$, respectively) is in $\mathcal{F}_{(\omega,\omega_0)}$ and, by hypothesis, also in $\mathcal{F}_{(\pi,\pi_0)}$. Thus, $\pi x = \pi x^{A'} = \pi_0$ which implies that $\pi_A = \pi_{A'} = 0$ (analogously, $\pi_B = \pi_{B'} = \pi_C = \pi_{C'} = \pi_D = \pi_{D'} = 0$).

Therefore, for all grid segments e in $\mathrm{GI}(P) - \{1, 2\}$, we have that $\pi_e = 0$. In Case 1, this implies that $\pi_1 = \pi_0$ while in Case 2 this implies that $\pi_2 = \pi_0$. We conclude that π is of the form $(\pi_0, \pi_0, 0, \ldots, 0)$ which implies that $\pi x \geq \pi_0$ is a scalar multiple of the original inequality and this completes the proof. □

Theorem 4.6 *Class II inequalities define facets of* $\mathcal{P}_{\mathcal{R}}$.

Proof: Again the validity comes from Theorem 4.1. Denoting by $\mathcal{F}_{(\omega,\omega_0)}$ the face defined

by an arbitrary Class II inequality in $\mathcal{P}_{\mathcal{R}}$, we have that $\mathcal{F}_{(\omega,\omega_0)} \neq \mathcal{P}_{\mathcal{R}}$ since the vector $\mathbb{1}_m \in \mathcal{P}_{\mathcal{R}} - \mathcal{F}_{(\omega,\omega_0)}$.

We consider the Steiner point i and grid segment 1, 2, 3 and 4 incident to it and arranged as in the previous proof. We show, w.l.o.g., that the Class II inequality $x_1 + x_2 - x_3 \geq 0$ defines a facet of $\mathcal{P}_{\mathcal{R}}$.

Assume the existence of a valid inequality $\pi x \geq \pi_0$ which defines the face $\mathcal{F}_{(\pi,\pi_0)}$ in $\mathcal{P}_{\mathcal{R}}$. Moreover, we suppose that the face $\mathcal{F}_{(\omega,\omega_0)} = \{x \in \mathcal{P}_{\mathcal{R}} \ : \ x_1 + x_2 - x_3 = 0\}$ is contained in $\mathcal{F}_{(\pi,\pi_0)}$. Using these facts, we show that the coefficients of vector π and π_0 are related in such a way that $\pi = \alpha\omega$ and $\pi_0 = \alpha\omega_0$ for some $\alpha \in \mathbb{R}_+$.

By Lemma 4.1, we know that $\pi_i = 0$ for all grid segments i external to the support rectangle of $x_1 + x_2 - x_3 \geq 0$. We now have to consider the components of π corresponding to the remaining grid segments.

Case 1: Let x and $\overline{x}$ be the incidence vectors of the solutions shown in Figure 11(a) and (b) respectively. Since x and $\overline{x}$ are in $\mathcal{F}_{(\omega,\omega_0)}$, we have that $\pi x = \pi\overline{x} = \pi_0$. We conclude that $\pi_4 = 0$.

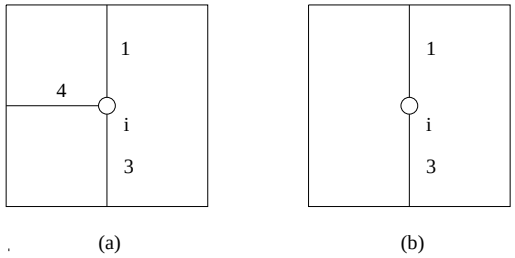

Figure 11: (a) A solution with incidence vector $x = (1, 0, 1, 1, \ldots, 1)$. (b) A solution with incidence vector $\overline{x} = (1, 0, 1, 0, 1, 1, \ldots, 1)$.

Case 2: Consider the solution in Figure 12 (a) whose incidence vector is $x = (1, 0, 1, 1, \ldots, 1)$. In (b) the axes of symmetry of this solution through the Steiner point i are shown.

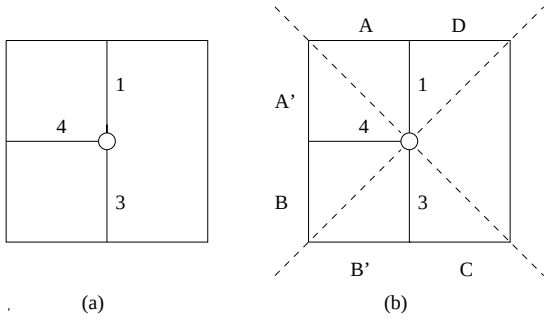

Figure 12: (a) A solution with incidence vector $x = (1, 0, 1, 1, \ldots, 1)$. (b) The axes of symmetry of the solution.

By removing the segment A (B,C,D) from the solution represented by x we obtain the incidence vector x^A (x^B,x^C,x^D) of another feasible solution. Since both x and x^A are in

$\mathcal{F}_{(\omega,\omega_0)}$, we have that $\pi x = \pi x^A = \pi_0$, which gives $\pi_A = \pi_{A'} = 0$. Analogously, it can be proved that $\pi_B = \pi_{B'} = \pi_C = \pi_D = 0$.

Case 3: Consider the solution represented in Figure 13 whose incidence vector is $x = (0, 1, \ldots, 1)$. By removing the segment D' (C') from the solution corresponding to x we obtain the vector $x^{D'}$ ($x^{C'}$) which is the incidence vector of another feasible solution. Both x and $x^{D'}$ ($x^{C'}$) lie on $\mathcal{F}_{(\omega,\omega_0)}$ and therefore, $\pi_{D'} = 0$ ($\pi_{C'} = 0$). Moreover, by comparing the value of πx for the solutions in Figure 12(a) and 13, we get $\pi_1 = \pi_2$.

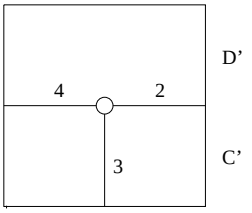

Figure 13: A solution with incidence vector given by $x = (0, 1, \ldots, 1)$.

Case 4: Let x be the incidence vector of the feasible partition where $x_i = 0$ for all $i \in \{1, 2, 3, 4\}$ and $x_i = 1$ for all $i \in \mathrm{GI}(P) \setminus \{1, 2, 3, 4\}$. We have that $x \in \mathcal{F}_{(\omega,\omega_0)}$ and therefore, $\pi x = \pi_0$. As we have already shown that $\pi_i = 0$ for all $i \in \mathrm{GI}(P) \setminus \{1, 2, 3\}$, we conclude that $\pi_0 = 0$. Now, taking for instance the solution in Figure 13, we can conclude that $\pi_3 = -\pi_2$ and this completes the proof since π is of the form $(\alpha, \alpha, -\alpha, 0, \ldots, 0)$. □

Further classes of facet defining inequalities are introduced below. They can be added to the formulation to make it stronger. The addition of these new inequalities to the original model is discussed later in Section 6.

Consider the point configuration depicted in Figure 14. Notice that points p_1, p_2 and p_3 are terminal points while p_4 is a Steiner point. Moreover, these points are vertices of a rectangle of GI(P).

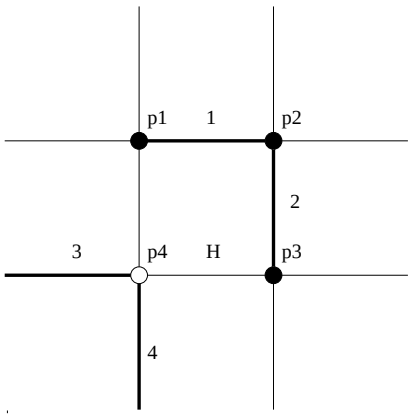

Figure 14: Point configuration of a Class III inequality.

The Class III inequality for Figure 14 is given by

$$x_1 + x_2 + x_3 + x_4 \geq 2 \tag{1}$$

There are $O(n)$ such inequalities and they all define facets as we show next.

Theorem 4.7 *Class III inequalities define facets of* $\mathcal{P}_\mathcal{R}$.

Proof: We show that the inequality is valid and the remaining of the proof is given in the Appendix. The proof of validity is divided into three cases. We assume that x is the incidence vector of an arbitrary feasible partition.

Case 1: $x_1 = 1$ and $x_2 = 0$. When x_2 is zero, one of the Class I inequalities at point p_3 forces x_H to be equals one which in turn, implies that x_3 and/or x_4 also takes value one to avoid an island or a knee at point p_4.

Case 2: $x_1 = 0$ and $x_2 = 1$. Notice that there is an axis of symmetry through points p_2 and p_4. Thus, the proof for this case is analogous to that of case 1 since segments 1 and 2 are symmetric.

Case 3: $x_1 = x_2 = 1$. The inequality is trivially satisfied.

Note that the case $x_1 = x_2 = 0$ is not allowed since there would be a Class I inequality violated at point p_2. □

Now consider four grid points in GI(P), one terminal and three Steiner, arranged like the configuration shown in Figure 15. The Class IV inequality is given by:

$$x_1 + x_2 + x_3 + x_4 \geq 1 \tag{2}$$

In Figure 15 we illustrate the support of a Class IV inequality. There are $O(n)$ such inequalities and the necessary and sufficient conditions under which they define facets of $\mathcal{P}_\mathcal{R}$ are given in the next theorem.

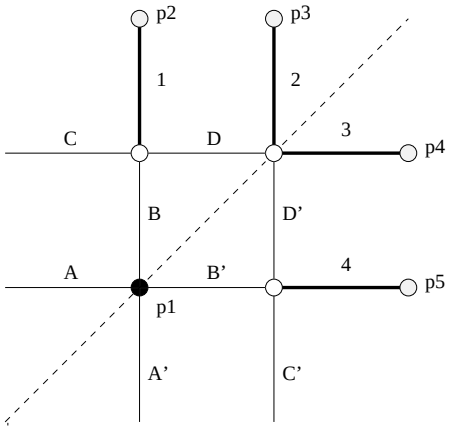

Figure 15: Support of a Class IV inequality. The points p_2, p_3, p_4 and p_5 are either terminal or Steiner. The dotted line represents the axis of symmetry of the support.

Theorem 4.8 *Every Class IV inequality is valid for $\mathcal{P}_{\mathcal{R}}$. It defines a facet of this polytope if and only if both pair of points (p_2, p_3) and (p_4, p_5) contain at least one Steiner point.*

Proof: We start by proving the validity. For this, we make use of Figure 15. Let x be the incidence vector of a feasible partition. If x_D or $x_{D'}$ is one, then x_2 or x_3 (or both) are one and the inequality is satisfied. So, assume that both x_D and $x_{D'}$ are zero. Since p_1 is a terminal point, at least one of the following relations must hold: $x_{A'} = x_B = 1$ or $x_A = x_{B'} = 1$. If $x_{A'} = x_B = 1$ ($x_A = x_{B'} = 1$) and $x_D = 0$ ($x_{D'} = 0$), then we must have $x_1 = 1$ ($x_4 = 1$) and, therefore, x satisfies the inequality. Thus, validity is proved.

We now proof necessity for the second part of the Theorem. Suficciency is proved in the Appendix.

Let $\omega x \geq \omega_0$ denote the Class IV inequality given in (2) and let $\mathcal{F}_{(\omega,\omega_0)} = \{x \in \mathcal{P}_{\mathcal{R}} : \omega x = \omega_0\}$ be the face defined by this inequality in $\mathcal{P}_{\mathcal{R}}$. Assume, by contradiction, that both p_2 and p_3 are terminal points (symmetry handles the case when both p_4 and p_5 are terminal points). When this occurs, every incidence vector $x \in \mathcal{F}_{(\omega,\omega_0)}$ must satisfy $x_e = 1$, where e is the segment with endpoints p_2 and p_3. This is necessary to satisfy the Class I inequalities in both terminal points since, if x is in $\mathcal{F}_{(\omega,\omega_0)}$, x_1 and x_2 cannot be both at one. But, this implies that $\mathcal{F}_{(\omega,\omega_0)}$ is contained in the hyperplane $x_e = 1$ and therefore inequality (2) is not facet defining. □

Figure 16 shows the point configuration in GI(P) which form the basis of the support of a Class V inequality. The corresponding Class V inequality is given by:

$$2\sum_{i=1}^{8} x_i + \sum_{i=9}^{12} x_i - \sum_{i=13}^{14} x_i \geq 6 \tag{3}$$

As for the previous classes of inequalities, there are $O(n)$ Class V inequalities. Below we prove that these inequalities define facets in $\mathcal{P}_{\mathcal{R}}$.

Theorem 4.9 *Class V inequalities define facets of $\mathcal{P}_{\mathcal{R}}$.*

Proof: As before, we show validity and complete the proof in the Appendix. Consider the support of a Class V inequality in Figure 16 and suppose that x is the incidence vector of an arbitrary feasible partition.

The basic idea in proving validity is to analyze the grid segments incident to the terminal points p_5 and p_7. Notice that, for any feasible partition, at each terminal point p the two horizontal and/or the two vertical segments incident to p belong to the partition. Thus, we split the proof in different cases according to which of these situations occur at points p_5 and p_7.

First, we rewrite the Class V inequality (3) in the following form:

$$2\sum_{i=1}^{8} x_i + (x_{11} + x_9 - x_{13}) + (x_{12} + x_{10} - x_{14}) \geq 6 \tag{4}$$

The terms in parenthesis are both nonnegative since they correspond to the left-hand side of Class II inequalities at the Steiner points p_4 and p_3 respectively. Thus, to prove

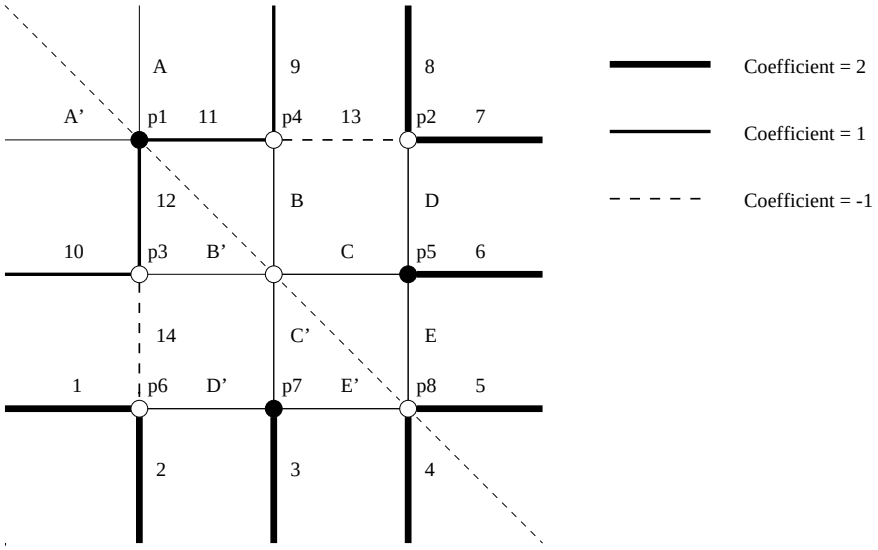

Figure 16: The support of a Class V inequality. The symmetry axis is represented by the dotted line.

validity it is enough to show that at least three segments from 1 to 8 belong to any feasible partition. This is what occurs in Cases 1 to 3 below.

Case 1: $x_D = x_E = x_{C'} = x_3 = 1$. We must have that at least one of the variables x_7 or x_8 equals one to avoid an island or a knee at point p_2. Analogously, we must have at least one of the variables x_4 or x_5 equals one to avoid an island or a knee at point p_8.

Case 2: $x_C = x_6 = x_{D'} = x_{E'} = 1$. Symmetric to Case 1.

Case 3: $x_D = x_E = x_{D'} = x_{E'} = 1$. To avoid an island or knee at point p_6, either x_1 or x_2 takes the value one. Moreover, as in Case 1, since $x_D = x_E = 1$, either x_7 or x_8 is one and either x_4 or x_5 is one.

Case 4: $x_C = x_6 = x_{C'} = x_3 = 1$. If $x_{13} = 1$ then $2(x_7 + x_8) \geq 2$ and $x_9 + x_{11} \geq 1$ which satisfies the inequality, since the two first terms in inequality (4) already sum up to 6. By symmetry, if $x_{14} = 1$ which implies that $2(x_1 + x_2) \geq 2$ and $x_{10} + x_{12} \geq 1$ and the inequality is satisfied. So, if there exists a solution violating the inequality (4) must satisfy $x_{13} = x_{14} = 0$. But Class I inequality at point p_1 implies that $x_{11} + x_{12} \geq 1$. If $x_{11} = 1$ ($x_{12} = 1$), since $x_{13} = 0$ ($x_{14} = 0$), then x_9 (x_{10}) must be equals one and the inequality holds (since, in this case, the the first term in inequality (4) is 4 and the second (third) term is 2). □

The support of an inequality for the last class of inequalities we introduce is illustrated in Figure 17. The Class VI inequality corresponding that Figure is given by:

$$\sum_{i=1}^{8} x_i \geq 2 \tag{5}$$

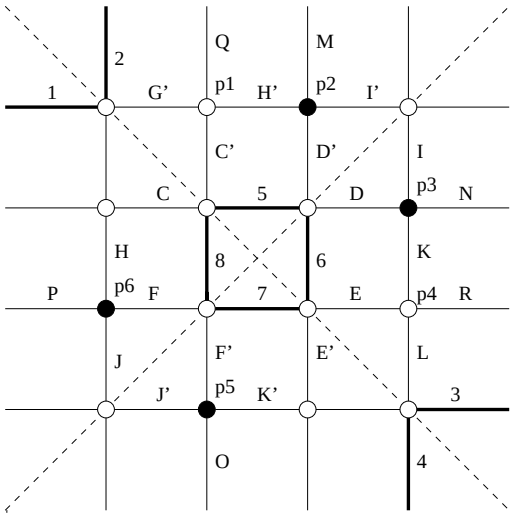

Figure 17: Support of a Class VI inequality. The two axis of symmetry are given by the dotted lines.

Again, the number of such inequalities is linear in $O(n)$ and they define facets of $\mathcal{P}_{\mathcal{R}}$ as it is shown below.

Theorem 4.10 *Class VI inequalities define facets of* $\mathcal{P}_{\mathcal{R}}$.

Proof: Only the validity part of the proof is given here. The proof is completed in the Appendix. The idea is to analyze the grid segments incident to the terminal points p_2, p_3, p_5, p_6 and to the Steiner points p_1 and p_4 (see Figure 17).

Assume that x is the incidence vector of an arbitrary feasible partition.

Case 1: $x_{F'} = x_O = x_{D'} = x_M = 1$. Since $x_{F'} = x_O = 1$, $x_7 + x_8 \geq 1$ and since $x_{D'} = x_M = 1$ then $x_5 + x_6 \geq 1$ and the inequality is satisfied.

Case 2: $x_F = x_P = x_D = x_N = 1$. Symmetric to Case 1.

Case 3: $x_F = x_P = x_{D'} = x_M = 1$. Since $x_F = x_P = 1$ we have that $x_7 + x_8 \geq 1$ and since $x_{D'} = x_M = 1$, we have that $x_5 + x_6 \geq 1$ and the inequality is satisfied.

Case 4: $x_{F'} = x_O = x_D = x_N = 1$. Symmetric to Case 3.

Case 5: $x_{J'} = x_{K'} = x_{H'} = x_{I'} = 1$. Since $x_{H'} = 1$, then $x_1 + x_2 + x_5 + x_8 \geq 1$. Since $x_{K'} = 1$, then $x_3 + x_4 + x_6 + x_7 \geq 1$.

Case 6: $x_H = x_J = x_I = x_K = 1$. Symmetric to Case 5.

Case 7: $x_H = x_J = x_{F'} = x_O = 1$. First note that $x_7 + x_8 \geq 1$. If x does not satisfy the inequality, we must have $x_{D'} = x_D = 0$, otherwise $x_5 + x_6 \geq 1$. However, in this situation, we must have $x_I = x_{I'} = x_{H'} = x_K = 1$. When $x_K = 1$, x must satisfy $x_E + x_L \geq 1$ (Class II inequality for point p_4) which implies that $x_3 + x_4 \geq 1$ or $x_6 + x_7 \geq 1$. Analogously, $x_{H'} = 1$ implies that $x_5 + x_8 \geq 1$ or $x_1 + x_2 \geq 1$. Thus, x satisfies the inequality.

Case 8: $x_{D'} = x_M = x_D = x_N = 1$. Symmetric to Case 7.

A simple enumeration shows that the cases given above cover all possible situations, since the two horizontal or the two vertical grid segments incident to terminal points both have to be in any feasible solution. This completes the proof. □

Inequalities in Classes III to VI can be used to strengthen the formulation presented in Section 4. The algorithmic aspects relative to the addition these inequalities in the formulation are discussed later. In the next section we present an alternative IP formulation of the RGP and compare the two models.

5 An Alternative Integer Programming Formulation for RGP: The Set Partitioning Model

A huge number of combinatorial problems can be formulated in terms of a Set Partitioning problem. The RGP problem belongs to this class. Before formulating the RGP as a Set Partitioning problem, let us briefly define the latter and give its IP formulation.

In the Set Partitioning problem we are giving a set $H = \{1, \ldots, m\}$ and a set $K = \{K_1, \ldots, K_n\}$ of subsets of H. If $J = \{1, \ldots, n\}$, the set $J^* \subseteq J$ defines a partition of H if $\bigcup_{j \in J^*} K_j = H$ and $\forall\, j, \ell \in J^*$, $j \neq \ell$, we have that $K_j \cap K_\ell = \emptyset$. If a cost c_j is associated to each subset K_j in K, the cost of the partition is computed as $\sum_{j \in J^*} c_j$. The goal is to find a partition with minimum cost. The problem can be easily modeled by the 0-1 IP below.

$$\begin{aligned} \text{Minimize} \quad & \sum_{j=1}^{n} c_j y_j \\ \text{Subject to} \quad & \sum_{j=1}^{n} a_{ij} y_j = 1, \quad i = 1, \ldots, m; \\ & y_j \in \{0, 1\}, \qquad j = 1, \ldots, n. \end{aligned}$$

where a_{ij} is one if $i \in K_j$ and zero otherwise. The variable y_j, $j \in J$, assumes a value of one if K_j belongs to the partition and zero otherwise.

In order to formulate the RGP as a Set Partitioning problem we have to set up the proper values for the a_{ij} and c_j coefficients. This depends on how we define the sets H and K which is done by introducing some further definitions.

Definition 5.1 *Let GI(P) be the induced grid corresponding to an instance of the RGP represented by an external rectangle R and a set P of terminal points. A rectangle whose sides lie on two consecutive vertical and horizontal lines of GI(P) (including the borders of R) is called a* canonical rectangle.

Figure 18 illustrates the above definition. Note that the number of canonical rectangles is $O(|P|^2)$.

Now, the sets H and K are defined as follows. Let $H = \{1, \ldots, m\}$ where m is the number of canonical rectangles in GI(P). Moreover, let $K = \{R_1, \ldots, R_q\}$ be the set of all rectangles with sides lying on the lines defining GI(P) (including the borders of R) and with

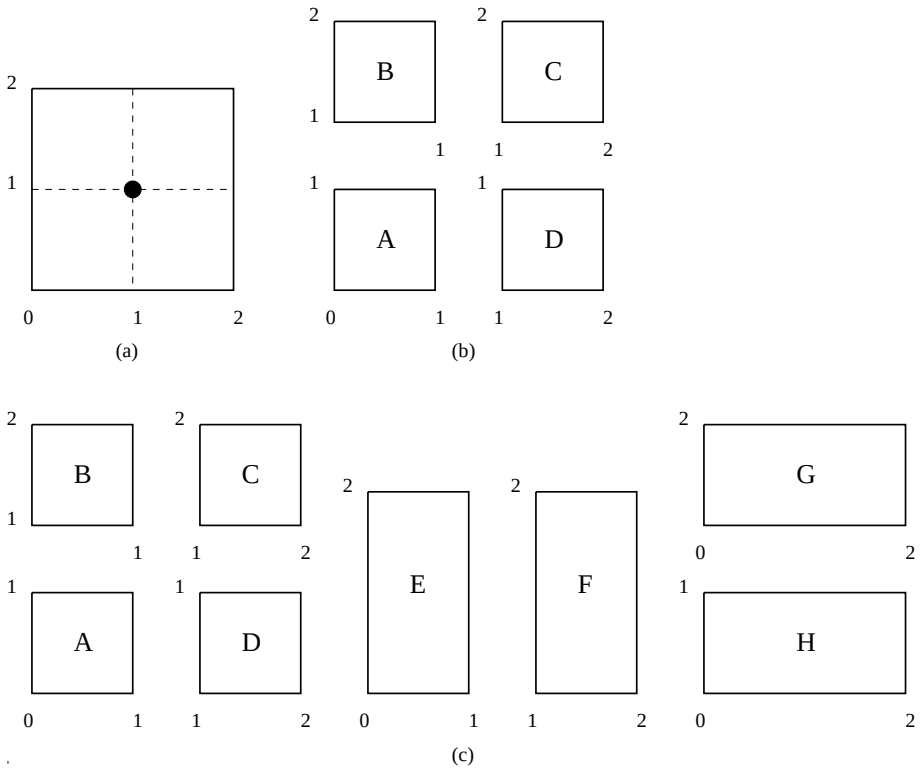

Figure 18: (a) Instance of the RGP. (b) Canonical rectangles in GI(P). (c) Feasible rectangles.

no terminal points in the interior. These rectangles are called *feasible* and there are $O(|P|^4)$ such ones. The K set of feasible rectangles can be easily seen to contain the set of canonical rectangles and each feasible rectangle can be viewed as the union of canonical rectangles (for instance, in Figure 18(c) the rectangle E is the union of the canonical rectangles A and B).

Clearly, any rectangular partition of R with respect to P can be seen as a partition of R into feasible rectangles. Assume that for every feasible rectangle R_j in K we define the cost c_j computed as the sum of the perimeter of R_j plus the sum of the length of the sides of R_j which lie on the boundary of R (see Figure 19). Thus, an IP formulation of the RGP as a Set Partitioning problem is obtained by setting:

$$y_j = \begin{cases} 1 & \text{if the feasible rectangle } R_j \text{ is in the partition,} \\ 0 & \text{otherwise.} \end{cases}$$

and

$$a_{ij} = \begin{cases} 1 & \text{if the feasible rectangle } j \text{ contains the canonical rectangle } i, \\ 0 & \text{otherwise.} \end{cases}$$

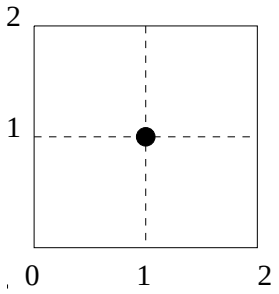

Figure 19: If R_j is the feasible rectangle with vertices at the points $(0,0),(1,0),(1,1),(0,1)$ the cost of R_j is given by $c_j = 6$.

In this formulation we have one equality constraint for each canonical rectangle and one variable for each feasible rectangle. Therefore, we have $O(|P|^2)$ constraints and $O(|P|^4)$ variables. If we denote by F_S the formulation with grid segment variables described in Section 4 and by F_R the formulation above with feasible rectangle variables, the optimal solutions of the two problems are related as follows.

Theorem 5.1 *Given a rectangle R and a set P of terminals in the interior of R, let x^* be an optimal integer solution with value Z^* obtained from F_S. Moreover, let y^* be an optimal integer solution with value W^* obtained from F_R. Then, $W^* = 2Z^* + 2Per(R)$, where $Per(R)$ is the length of the perimeter of R.*

Proof: Immediate, since in Z^* only the length of the grid segments are computed while, from the definition of the c_j's, in W^* the length of each grid segment is counted twice (once

for each of the rectangles of the partition it belongs to) and the length of the boundary of R is also counted twice. □

The next theorem compares the bounds obtained by solving the linear relaxations of F_S and F_R and shows that the second formulation is stronger.

Theorem 5.2 *Let W^* be the optimal value of the linear relaxation of F_R and Z^* be the optimal value of the linear relaxation of F_S for a given instance of the RGP. Then, $W^* \geq 2Z^* + 2Per(R)$, where $Per(R)$ is the length of the perimeter of R. Moreover, the inequality may be verified strictly.*

Proof: To show that $W^* \geq 2Z^* + 2\text{Per}(R)$ it is enough to show that, given any vector y satisfying the constraints of F_R, y can be transformed into a vector x satisfying the constraints in F_S. Given this transformation, the cost of x^* must be at least Z^*, since Z^* was assumed to be the optimal value of the linear relaxation of F_S.

Thus, starting from a vector y satisfying the constraints of F_R except possibly the integrality constraints, let us obtain a vector x such that: (i) x satisfies both Class I and Class II inequalities and (ii) for each grid segment s we have that $0 \leq x_s \leq 1$.

Let Γ_s be the set of feasible rectangles which have the grid segment s as part of one of its sides. Let x_s be computed such that: $x_s = \frac{1}{2}\sum_{k\in\Gamma_s} y_k$. We now prove that x satisfies the constraints of the linear relaxation of F_S.

Case 1: $x_s \geq 0$, for all $s \in \text{GI}(P)$. Trivial since $y \geq 0$.

Case 2: $x_s \leq 1$, for all $s \in \text{GI}(P)$. The grid segment s is the common side of two canonical rectangles R_s^1 and R_s^2. Since, from the formulation F_R, $\sum_{j=1}^{q} a_{R_s^1,j} y_j = 1$ and $\sum_{j=1}^{q} a_{R_s^2,j} y_j = 1$ we have that

$$x_s = \frac{1}{2}\sum_{k\in\Gamma_s} y_k \leq \frac{1}{2}(\sum_{j=1}^{q} a_{R_s^1,j} y_j + \sum_{j=1}^{q} a_{R_s^2,j} y_j) \leq 1.$$

The first inequality in the expression above is justified by the fact that some rectangles that cover R_s^1 and R_s^2 do not have s as part of their sides.

Case 3: Class I inequality $x_{i(1)} + x_{i(2)} \geq 1$ for all terminal point i. The proof uses the notation presented in Figure 20. Let us denote by $\sum_{i,j}$ the sum of all components in y associated to feasible rectangles covering both R^i and R^j.

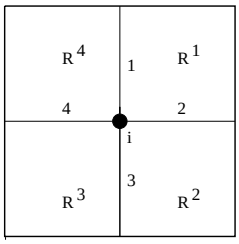

Figure 20: Notation for the proof of Case 3 of Theorem 5.2.

The values of $x_{i(1)}$ and $x_{i(2)}$ are given by:

$$x_{i(1)} = \frac{1}{2}(\sum_{1,1} + \sum_{1,2} + \sum_{3,4} + \sum_{4,4});$$

$$x_{i(2)} = \frac{1}{2}(\sum_{1,1} + \sum_{1,4} + \sum_{2,2} + \sum_{2,3}).$$

Hence, we have that:

$$x_{i(1)} + x_{i(2)} = \sum_{1,1} + \frac{1}{2}(\sum_{1,2} + \sum_{2,2} + \sum_{2,3}) + \frac{1}{2}(\sum_{1,4} + \sum_{3,4} + \sum_{4,4}).$$

Since the constraints in F_R for the canonical rectangles R^2 and R^4, respectively, imply that the first and second summations in parenthesis to be one, and $\sum_{1,1} \geq 0$, we obtain:

$$x_{i(1)} + x_{i(2)} = 1 + \sum_{1,1} \geq 1.$$

Case 4: Class II inequality $x_{i(1)} + x_{i(2)} - x_{i(3)} \geq 0$ for all Steiner point i. The proof uses the notation presented in Figure 21.

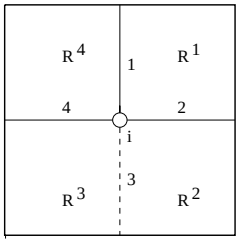

Figure 21: Notation for the proof of Case 4 of Theorem 5.2.

For $i \in \{1,2,3,4\}$, let C_E^i be the set of all feasible rectangles covering the canonical rectangle R^i. Moreover, let C^i be the subset of rectangles in C_E^i not covering at least one of the canonical rectangles R^j, for $j \in \{1,2,3,4\}$ and $j \neq i$.

From the previous observation, we conclude that $\sum_{j \in C^i} y_j$, for every $i = 1, \ldots, 4$, is equal to a constant α. Moreover, $\alpha \leq 1$ since $\sum_{j \in C^i} y_j \leq \sum_{j \in C_E^i} y_j = 1$. Thus, for a fixed index r in $\{1,2,3,4\}$, $\sum_{k \in C^r} y_k$ can be expressed in terms of the $\sum_{i,j}$ as defined before. For instance,

$$\sum_{j \in C^3} y_j = \sum_{2,3} + \sum_{3,3} + \sum_{3,4} = \alpha \leq 1$$

$$\sum_{j \in C^4} y_j = \sum_{1,4} + \sum_{3,4} + \sum_{4,4} = \alpha \leq 1$$

To compute the LHS of the Class II inequality we use the fact that the terms involved in this expression are given by:

$$x_{i(1)} = \frac{1}{2}(\sum_{1,1} + \sum_{1,2} + \sum_{3,4} + \sum_{4,4})$$

$$x_{i(2)} = \frac{1}{2}(\sum_{1,1} + \sum_{1,4} + \sum_{2,2} + \sum_{2,3})$$

$$-x_{i(3)} = -\frac{1}{2}(\sum_{1,2} + \sum_{2,2} + \sum_{3,3} + \sum_{3,4})$$

hence,

$$\begin{aligned} x_{i(1)} + x_{i(2)} - x_{i(3)} &= \sum_{1,1} + \frac{\sum_{1,4} + \sum_{2,3} + \sum_{4,4} - \sum_{3,3}}{2} \\ &= \sum_{1,1} + \frac{(\sum_{1,4} + \sum_{4,4}) + \sum_{2,3} - \sum_{3,3}}{2} \\ &= \sum_{1,1} + \frac{\alpha - \sum_{3,4} + \sum_{2,3} - \sum_{3,3}}{2} \\ &= \sum_{1,1} + \frac{(\alpha - \sum_{3,4} - \sum_{3,3}) + \sum_{2,3}}{2} \\ x_{i(1)} + x_{i(2)} - x_{i(3)} &= \sum_{1,1} + \sum_{2,3} \geq 0. \end{aligned}$$

To show that the inequality $W^* \geq 2Z^* + 2\text{Per}(R)$ is not necessarily satisfied at equality, and therefore, that F_R is a stronger formulation than F_S, it suffices to exhibit an instance where the inequality holds. This is done in Figure 22. The values of the variables associated to the grid segments represented by dotted (full) lines are 0.5 (1.0). The optimal values of the linear relaxations of F_S and F_R are respectively 14.5 and 15.0. □

6 Computational Experiments

In this section we present the computational experiments that we have carried out with the exact algorithms for the RGP based on the IP formulations introduced in the previous sections. Initially, we briefly describe the set of instances used in our tests and analyze the performance of some known heuristics on this data set. Subsection 6.2 is devoted to the discussion of implementation details and results of the Branch-and-Bound (**B&B**) and Branch-and-Cut (**B&C**) algorithms we have developed to solve the segment model from Section 4. Finally, in Subsection 6.3, we discuss the implementation issues and the results of the Branch-and-Price (**B&P**) algorithm we have developed for the Set Partitioning formulation from Section 5.

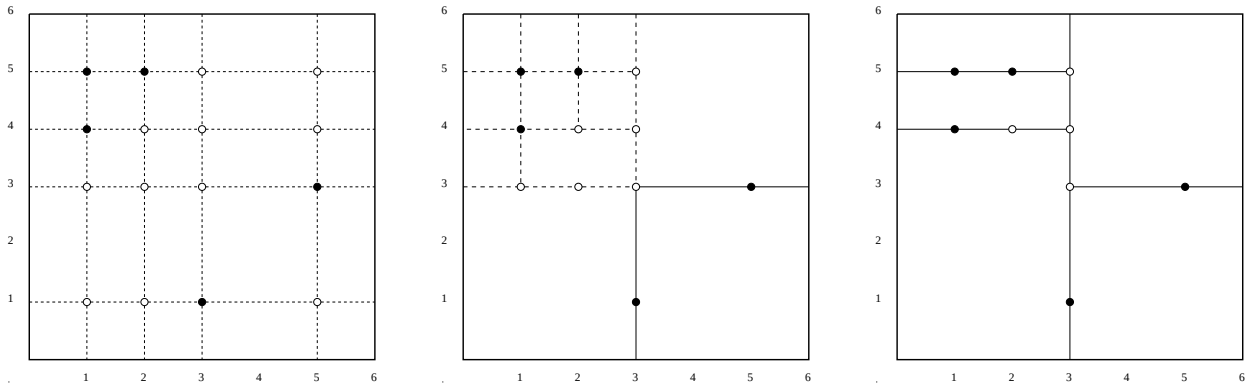

Figure 22: (a) Instance of the RGP for the proof of Theorem 5.2. (b) Optimal solution of the linear relaxation of F_S. (c) Optimal solution of the linear relaxation of F_R.

All tests have been run on a SPARC 1000 machine with 392 Mb of RAM under Solaris 2.5 operating system. The programs are implemented in `C` language and `CPLEX` version 3.0 ([1]) is used as the Linear Programming (LP) solver.

6.1 Instances and heuristic solutions

Two classes of instances have been generated. In the first one the set P of terminal points is corectilinear while in the second P is noncorectilinear. The external rectangle R has size either 20×20 or 50×50. There are 35 instances, 25 of which with noncorectilinear points. Points are given by integer coordinates uniformly distributed in the interior of R.

We have implemented the approximation algorithm described in [2], here denoted by DPS86, so as to have an incumbent solution at the beginning of the (implicit) enumeration algorithms. This approximation algorithm produces the optimal guillotine partition and is known to outperform the algorithms described in [5], [4] and [7]. All instances have been solved within a few seconds and we have observed that the processing time, for fixed $|P|$, tend to increase significantly (even by a factor of 10) when the set of terminal points is noncorectilinear.

6.2 Branch-and-Bound and Branch-and-Cut algorithms

We now discuss the results we have obtained with **B&B** and **B&C** algorithms based on the model introduced in Section 4. The results are summarized in Tables 3 to 9. In these tables, the column headings **#cons**, **#var**, **opt**, **#nodes**, **#LPs**, **#cuts** stand for, respectively: the number of constraints in the model, the number of variables in the model, the optimal value, the number of nodes opened in the enumeration procedure, the number of linear programs solved and number of cuts (inequalities) founded in the cutting planes phase.

In the table cells containing the optimal value of the relaxation for both IP models, the symbol (I) is used to indicate that the solution corresponding to this value is integral.

We use some classical techniques to implement the search procedures. Thus, the selection of the next node to be explored in the enumeration tree follows the *best bound* strategy. The *branching rule* selects the *most fractional* variable, i.e., the one whose value is closest to 0.5 . The **B&C** implementation is based on the description presented by Jünger et al. in [9]. In the latter algorithm, we branch on a variable whenever the LP value varies less than 0.01% after the execution of 10 consecutive iterations. The goal is to escape from the *tailing off* effect during the *cutting plane* phase.

Initially, we compare three different algorithms to solve the instances in the 20×20 square. These algorithms are: (a) **B&B** on the *basic* segment formulation (with inequalities in Classes I and II); (b) **B&B** using the *full* segment formulation with all the inequalities in Classes I to VI and (c) **B&C** starting with the basic formulation and with inequalities in Classes III to VI separated and added during the iterations, i.e., when they are found to be violated by the fractional solution of the LP being solved at the current node of the enumeration tree. Since the number of possibly violated inequalities is $O(|P|)$, the separation is done by enumeration.

From Tables 3, 4 and 5 (6, 7 and 8), it is clear that the algorithm (b) outperforms algorithms (a) and (c). The addition of all inequalities in Classes III, IV, V and VI slightly increases the time needed for solving the LPs (compare the columns **Relaxation/time** in Tables 3 and 4). This explains why the **B&C** algorithm in (c), which uses these inequalities as cutting-planes, is not competitive with the algorithm in (b). On the other hand, the results give a clear indication that the inequalities in Classes III to VI are very helpful to describe the portion of $\mathcal{P}_{\mathcal{R}}$ on which lies an optimal solution. As an evidence of this fact, in the last rows of Tables 3 and 4, for $|P| = 200$, we see that algorithm (b) explores about 1400 times less nodes of the enumeration tree than algorithm (a) which, in consequence, has been more than 200 times slower.

These reductions obtained by algorithm (b) (relative to algorithm (a)) in the CPU time and in the number of nodes explored in the enumeration tree, are less impressive when we look at the noncorectilinear instances. Nevertheless, they still remain important. If, for example, we consider the largest instance ($|P| = 19$) in Tables 6 and 7, we see that algorithm (b) have run 7 times faster than algorithm (a). Undoubtedly, the noncorectilinear instances are much harder to solve with **B&B** than the corectilinear ones.

Notice that the inequalities in Classes III and IV are those that appear more often (except, obviously, Class III inequalities for noncorectilinear instances). We have identified very few inequalities in Class V and no inequalities in Class VI.

Our essays to exactly solve larger instances for the noncorectilinear case have failed. The demand for computational resources (CPU time and memory space) when solving such instances is prohibitively large. We have restricted ourselves to solve the linear relaxations of instances with $20 \leq |P| < 40$ in order to get lower bounds (see Table 9). As for the previous instances, the inclusion of the inequalities in Classes IV and V has increased the lower bounds provided by the linear relaxations. For noncorectilinear instances, this increasing has been of up to 7% independently of $|P|$, while it has been limited to 3% for the smaller corectilinear case.

In Tables 3, 6 and 9 the value of the solution obtained by the best known approximation algorithm for each of the tested instances is presented (columns denoted by **DPS86**). In the

average, the approximate solution is 10% off the optimum and, worse, it has never reached the optimal value. Later in this section, we will see that, in the average, the lower bounds obtained with the *full* segment model are also at the same distance from the optimum.

Instance	DPS86		Relaxation				*Branch-and-Bound*		
$\|P\|$	value	time	#cons	#var	value	time	opt	#nodes	time
20	112	2s	1376	391	101.71	7s	108	176	2m27s
35	154	2s	2036	577	140.87	10s	145	99	1m13s
50	196	3s	2536	721	172.58	25s	176	62	1m40s
80	229	9s	2568	760	207(I)	12s	207	1	12s
100	259	8s	2488	760	236.89	16s	239	50	51s
120	285	12s	2408	760	257.75	13s	264	3011	13m19s
150	307	10s	2288	760	280.25	12s	283	120	1m00s
170	324	9s	2208	760	300.09	10s	303	173	57s
190	337	7s	2128	760	305.44	8s	312	44716	1h35m14s
200	341	13s	2088	760	314.50	9s	321	36927	1h23m24s

Table 3: Instances with corectilinear points for a 20×20 rectangle. *Basic* segment model.

Instance	Relaxation		*Branch-and-Bound*		
$\|P\|$	value	time	#nodes	time	inequalities
20	103.92	5s	38	50s	46(IV)
35	142.22	15s	43	1m04s	91(IV)/1(V)
50	174.17	21s	9	31s	5(III)/111(IV)/1(V)
80	-	-	-	-	-
100	238.00	15s	2	15s	17(III)/146(IV)/4(V)
120	261.34	14s	95	1m50s	32(III)/128(IV)/2(V)
150	282.09	19s	2	19s	49(III)/117(IV)/3(V)
170	301.57	13s	17	17s	78(III)/79(IV)/4(V)
190	309.72	7s	126	43s	83(III)/69(IV)
200	318.67	16s	25	21s	108(III)/65(IV)/2(V)

Table 4: Instances with corectilinear points for a 20×20 rectangle. *Full* segment model.

6.3 Branch-and-Price algorithm

A Branch-and-Price algorithm is an algorithm which embeds a column generation phase into a branch-and-bound framework. Our **B&P** algorithm has been implemented using the package MINTO (*Mixed INTeger Optimizer*) [14]. MINTO provides an environment for quick development of Branch-and-Price algorithms.

As for any column generation algorithm, there are some points that must be addressed

Instance	*Branch-and-Cut*			
$\|P\|$	#nodes	#LPs	#cuts	time
20	106	64	26(IV)	1m08s
35	98	58	24(IV)	1m04s
50	26	24	4(III)/38(IV)/1(V)	47s
80	1	1	-	12s
100	4	5	13(III)/8(IV)	12s
120	268	156	25(III)/32(IV)	3m55s
150	14	12	21(III)/6(IV)	17s
170	148	81	47(III)/8(IV)	1m18s
190	1034	536	54(III)/11(IV)	8m07s
200	94	59	56(III)/6(IV)	1m01s

Table 5: Instances with corectilinear points for a 20×20 rectangle. *Basic* segment model used as the initial formulation and inequalities in Classes III to VI added when necessary in a **B&C**.

Instance	DPS86		Relaxation				*Branch-and-Bound*		
$\|P\|$	value	time	#cons	#var	value	time	opt	#nodes	time
15	120	$< 1s$	1740	480	103.85	8s	110	120	1m52s
16	124	$< 1s$	1984	544	100.90	13s	113	1722	37m00s
17	122	1s	2244	612	107.69	19s	119	4193	1h44m24s
18	134	1s	2520	684	108.41	21s	124	4002	1h58m12s
19	140	3s	2812	760	115.11	38s	127	8795	7h14m35s

Table 6: Instances with noncorectilinear points for a 20×20 rectangle. *Basic* segment model.

Instance	Relaxation		*Branch-and-Bound*		
$\|P\|$	value	time	#nodes	time	inequalities
15	106.38	10s	39	59s	52(IV)
16	106.55	14s	434	13m17s	52(IV)/1(V)
17	111.74	18s	769	23m48s	56(IV)
18	114.05	20s	3600	1h55m48s	57(IV)
19	119.63	49s	804	55m57s	66(IV)

Table 7: Instances with noncorectilinear points for a 20×20 rectangle. *Full* segment model.

Instance	*Branch-and-Cut*			
$\|P\|$	#nodes	#LPs	#cuts	time
15	102	60	38(IV)	2m04s
16	1070	605	45(IV)/1(V)	41m48s
17	1702	979	52(IV)	1h18m54s
18	7340	4189	52(IV)	6h48m52s
19	1550	791	60(IV)	2h42m48s

Table 8: Instances with noncorectilinear points for a 20×20 rectangle. *Basic* segment model used as the initial formulation and the inequalities in Classes IV, V and VI added when necessary in a **B&C**.

Instance	DPS86		Relaxation				
$\|P\|$	value	time	#cons	#var	value	time	inequalities
20	341	3s	3120	840	282.01	32s	66(IV)
21	358	5s	3444	924	294.64	50s	71(IV)
22	365	1s	3784	1012	298.47	48s	74(IV)/1(V)
23	392	3s	4140	1104	305.67	1m13s	82(IV)
24	398	8s	4512	1200	327.63	1m24s	87(IV)
25	397	8s	4900	1300	320.85	2m10s	88(IV)
26	421	3s	5304	1404	334.53	2m36s	94(IV)
27	424	9s	5724	1512	332.55	2m58s	100(IV)
28	437	6s	6160	1624	342.61	3m20s	102(IV)
29	435	12s	6612	1740	339.58	3m33s	106(IV)
30	435	11s	7080	1860	344.90	4m57s	107(IV)
31	449	15s	7564	1984	364.97	5m30s	114(IV)
32	484	17s	8064	2112	335.95	6m44s	114(IV)
33	482	18s	8580	2244	360.50	10m31s	120(IV)
34	475	17s	9112	2380	369.14	9m20s	124(IV)
35	486	21s	9660	2520	369.06	13m48s	124(IV)
36	491	24s	10224	2664	371.48	13m00s	132(IV)
37	493	22s	10804	2812	359.27	17m13s	132(IV)
38	505	35s	11400	2964	404.54	17m33s	140(IV)
39	526	38s	12012	3120	393.29	23m57s	146(IV)

Table 9: Instances with noncorectilinear points for a 50×50 rectangle. *Full* segment model.

to obtain a good implementation. The first point is the set of initial columns that are added to the restricted master problem. For the RGP we have decided to start with the columns corresponding to all canonical rectangles (which already ensures feasibility) and also those corresponding to the rectangles that form the optimal guillotine partition (see Section 2). The pricing subproblem which generates the column(s) to be added to the current LP can be solved in polynomial time since the total number of columns is $O(|P|^4)$. We actually solve this problem by enumeration, but this point may deserve further investigations since the time spent in solving the pricing subproblem is considerably large. The number of columns generated at each iteration is discussed later. The *branching rule* we adopt is also classical and it is based on the strategy proposed by Ryan and Foster [13] for Set Partitioning Problems.

Below we discuss the computational results we have obtained with a **B&P** algorithm based on the set partitioning model for RGP and introduced in Section 5.

In Tables 10 to 14 the column headings **LB**, **opt**, **#nodes**, **time**, **#icols**, **#cons** and **#cols** stand for, respectively: the lower bound obtained from the linear relaxation at the root node of the enumeration tree, the optimal value, the number of nodes visited in the enumeration tree, the CPU time needed to prove optimality, the number of columns in the *restricted master LP* at the end of the **B&P** procedure, the number of constraints in the model and the number of variables (columns) in the *master LP* (complete set partitioning formulation).

In the experiments reported in Tables 10 and 11, and in Tables 12 and 13 we have investigated the behavior of the **B&P** algorithm with respect to two different strategies to add columns to the *restricted master LP*. It is clear that the addition of multiple columns at each iteration leads to a much better performance of the algorithm than the addition of a single column with minimum reduced cost. From these tables, it is clear that most variables generated by the addition of multiple columns are actually useless.

As for the best **B&B** algorithm from the previous section, due to limitations on computational resources, the **B&P** algorithm has not been able to obtain the exact solution of 40-point noncorectilinear instances on a 50×50 square. Nevertheless, as it is shown in Table 14, the **B&P** algorithm solves all instances with $20 \leq |P| < 40$ in less than 20 hours of CPU. This has not been possible for the **B&B** algorithm.

The lower bounds provided by the linear relaxation of the set partitioning model are remarkably good and significantly better than those coming from the segment model. Notice that most of the tested instances have been solved by simple column generation, i.e., at the root node of the **B&P** enumeration tree. In all but 7 of the 35 instances solved by the **B&P** algorithm, the optimal solution of the linear relaxation is integral. In 4 out of the 7 instances for which we end up with an optimal fractional solution, the optimal value is integral and, among these 4 exceptions, in 2 instances the lower bound rounded up is precisely the optimal value (remind that by construction the costs are integer).

Despite the better quality of the bounds produced by the set partitioning model, the bounds provided by the segment model are also of good quality and they can be computed much faster. Regarding the overall CPU times, the **B&P** algorithm with the addition of multiple columns at each iteration is usually faster than the best **B&B** algorithm we have implemented. For the smaller instances in a 20×20 square, less than 10 minutes of CPU

is enough for this algorithm to prove optimality. However, it is also the case for the **B&P** algorithm that the noncorectilinear instances are harder to solve.

Instance	*Branch-and-Price*					*Master LP*	
$\|P\|$	LB	opt	#nodes	time	#icols	#cons	#cols
20	108(I)	108	1	30s	1956	210	5196
35	145(I)	145	1	1m22s	2740	306	8116
50	176(I)	176	1	3m18s	3611	380	11004
80	207(I)	207	1	2m43s	3658	400	10157
100	239(I)	239	1	2m47s	3387	400	9591
120	264(I)	264	1	2m27s	3535	400	9269
150	283(I)	283	1	2m28s	3579	400	8809
170	303(I)	303	1	2m14s	3498	400	8578
190	312(I)	312	1	2m35s	3494	400	8529
200	321(I)	321	1	2m23s	3501	400	8385

Table 10: Instances with corectilinear points for a 20×20 rectangle. Results for the strategy of adding at most 100 columns to the *restricted master LP*, at each iteration of the column generation algorithm.

Instance	*Branch-and-Price*			
$\|P\|$	LB	#nodes	time	#icols
20	108(I)	1	17m30s	585
35	145(I)	1	54m42s	846
50	176(I)	1	2h04m59s	1137
80	207(I)	1	1h53m54s	1105
100	239(I)	1	1h52m40s	1127
120	264(I)	1	2h00m00s	1199
150	283(I)	1	1h44m34s	1140
170	303(I)	1	1h49m26s	1169
190	312(I)	1	1h45m39s	1152
200	321	46	2h35m05s	1455

Table 11: Instances with corectilinear points for a 20×20 rectangle. Results for the strategy of adding only a column of minimum reduced cost to the *restricted master LP*.

7 Conclusions and Future Investigations

In this paper we introduce two different IP models for the RGP. Our goal is to solve this problem exactly by using some standard IP techniques. The first model, called the *segment model*, is investigated from a polyhedral point of view. Several classes of facet

Instance	*Branch-and-Price*					*Master LP*	
$\|P\|$	LB	opt	#nodes	time	#icols	#cons	#cols
15	110(I)	110	1	1m12s	2319	256	7262
16	113(I)	113	1	1m50s	2943	289	9292
17	117.67	119	27	8m04s	4131	324	11131
18	124(I)	124	1	4m47s	3860	380	13319
19	127(I)	127	1	6m50s	4469	400	15994

Table 12: Instances with noncorectilinear points for a 20×20 rectangle. Results for the strategy of adding at most 100 columns to the *restricted master LP*, at each iteration of the column generation algorithm.

Instance	*Branch-and-Price*			
$\|P\|$	LB	#nodes	time	#icols
15	110(I)	1	35m38s	730
16	113(I)	1	1h05m17s	864
17	117.67	27	1h51m24s	1080
18	124(I)	1	2h21m12s	1080
19	127(I)	1	3h35m54s	1247

Table 13: Instances with noncorectilinear points for a 20×20 rectangle. Results for the strategy of adding only a column of minimum reduced cost to the *restricted master LP*.

Instance	*Branch-and-Price*					*Master LP*	
$\|P\|$	LB	opt	#nodes	time	#icols	#cons	#cols
20	311(I)	311	1	8m27s	4888	441	18731
21	323(I)	323	1	12m03s	5426	484	22214
22	331	331	2	17m47s	6095	529	26286
23	326(I)	326	1	21m47s	6513	576	28434
24	367(I)	367	1	32m09s	7492	625	32855
25	356(I)	356	1	44m59s	8284	676	37952
26	371(I)	371	1	1h02m38s	9006	729	43508
27	370(I)	370	1	1h24m36s	10115	784	47767
28	378(I)	378	1	1h52m35s	10590	841	54646
29	387(I)	387	1	2h31m17s	11360	900	62133
30	387	387	2	3h46m47s	20039	961	69612
31	410(I)	410	1	1h44m06s	20139	1024	76269
32	410(I)	410	1	2h12m45s	21735	1089	90257
33	423	423	3	7h18m57s	24298	1156	94713
34	418(I)	418	1	3h30m37s	24764	1225	104149
35	434.50	435	3	5h28m10s	28556	1296	116590
36	439.50	440	3	9h31m04s	28472	1369	123787
37	439(I)	439	1	7h38m26s	32082	1444	149378
38	457	457	2	17h44m47s	32983	1521	143874
39	462(I)	462	1	8h15m14s	34167	1600	157432

Table 14: Instances with noncorectilinear points for a 50×50 rectangle. Results for the strategy of adding at most 500 columns to the *restricted master LP*, at each iteration of the column generation algorithm.

defining inequalities are introduced for the convex hull of the incidence vectors of feasible partitions. These inequalities are tested computationally both by adding them all from scratch and running a pure **B&B** algorithm and also by using them as cutting planes in a **B&C** algorithm. Our experiments on a randomly generated data set have shown that the **B&B** algorithm outperforms the **B&C** one. We observe that noncorectilinear instances tend to be more difficult with this approach than the corectilinear ones.

A second model, based on a set partitioning formulation of RGP, is introduced and compared to the segment model both theoretically and practically. From the theoretical point of view, we prove that the lower bounds provided by the linear relaxation of the set partitioning model dominate those coming from the linear relaxation of the segment model. To solve the set partitioning model we have implemented a **B&P** algorithm. The computational experiments show that the better quality of the set partitioning bounds leads to significant saves in CPU time when compared to the best **B&B** algorithm, especially for noncorectilinear instances.

We have also implemented the best approximation heuristic currently available in the literature ([2]). For all instances for which we have proved optimality, the approximation algorithm failed to produce an optimal solution. Usually the approximated value is about 10% off the optimum which is also the average distance of the lower bound provided by the linear relaxation of the *full* segment model (see 6.2 for details). The set partitioning model has a remarkable performance in what refers to the lower bounds computed from its linear relaxation. In all but one instance, it attains the optimal value (possibly after rounding it up).

Our experiments show that the IP models we introduce can be successfully applied to solve medium-sized instances to optimality for corectilinear points. It is worth noting that larger Set Partitioning models can possibly be solved by using more elaborate IP algorithms which have successfully been applied to crew scheduling problems (cf., [8]). The noncorectilinear case remains difficult to solve but using the set partitioning model and the **B&P** algorithm, we have solved instances with up to 39 terminal points. It is worth noting that the status of the noncorectilinear RGP problem is still open, though it is conjectured to be in $\mathcal{NP}$-hard ([5]).

Immediate extensions of our results can be made if we allow R to represent any rectilinear polygon and we include more general (but still rectilinear) kind of holes in the interior of R (and not only points). Further polyhedral investigations on the segment model may turn it more competitive so, its use should not be discarded a priori, despite the apparent superiority demonstrated by the set partitioning model in our computational results. Even restricted to the facet defining inequalities that are known, the segment model can be used to quickly compute lower bounds of good quality.

We strongly believe that the knowledge of optimal solutions for some reasonable sized instances of the problem may be helpful in understanding the geometric properties that must be satisfied by such solutions. Both models we introduce can be easily generated to serve as an input for commercial LP-solvers such as CPLEX. Thus, anyone interested in investigating those optimality properties is able to compute optimal solutions with a little effort. This is the direction we are currently developing our research on this problem.

Finally, we hope that works like this one can stimulate the cooperation between the

fields of mathematical programming and discrete computational geometry. We believe that this cooperation will be especially fruitful for geometric partitioning problems.

Acknowledgments

The proof of Theorem 3.2 is due to Prof. Dr. Pedro J. de Rezende.

Appendix

Proof of Theorem 4.7: Denote by $\omega x \geq \omega_0$ the inequality $x_1 + x_2 + x_3 + x_4 \geq 2$ and let $\mathcal{F}_{(\omega,\omega_0)} = \{x \in \mathcal{P}_{\mathcal{R}} : \omega x = \omega_0\}$ the face defined by it. Notice that $\mathcal{F}_{(\omega,\omega_0)} \neq \mathcal{P}_{\mathcal{R}}$ since the point $\mathbb{1}_m \in \mathcal{P}_{\mathcal{R}}$, and $\mathbb{1}_m \notin \mathcal{F}_{(\omega,\omega_0)}$. Assume that $\pi x \geq \pi_0$ is a valid inequality for $\mathcal{P}_{\mathcal{R}}$ such that $\mathcal{F}_{(\omega,\omega_0)} \subseteq \mathcal{F}_{(\pi,\pi_0)} = \{x \in \mathcal{P}_{\mathcal{R}} : \pi x = \pi_0\}$. We wish to show that $\pi = \alpha\omega$ and $\pi_0 = \alpha\omega_0$ for some $\alpha \in \mathbb{R}_+$.

By Lemma 4.1, we know that $\pi_i = 0$ for all grid segments i external to the support rectangle of $x_1 + x_2 + x_3 + x_4 \geq 2$. We now have to consider the components of π corresponding to the remaining grid segments.

Case 1: Consider the solution illustrated in Figure 23 whose incidence vector belongs to $\mathcal{F}_{(\omega,\omega_0)}$.

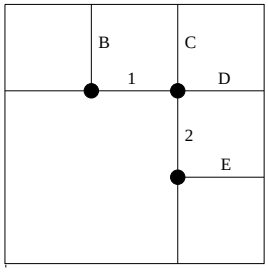

Figure 23: A solution with incidence vector x.

If we remove $B(C, D, E)$ from the solution represented by x we obtain a new feasible solution whose incidence vector $x^B(x^C, x^D, x^E$ respectively) is in $\mathcal{F}_{(\omega,\omega_0)}$. Thus, $\pi x = \pi x^B = \pi_0$ which implies that $\pi_B = 0$ (analogously, $\pi_C = \pi_D = \pi_E = 0$).

Case 2: Consider the solution illustrated in Figure 24 whose incidence vector belongs to $\mathcal{F}_{(\omega,\omega_0)}$.

If we remove $A(F, H)$ from the solution represented by x we obtain a new feasible solution whose incidence vector $x^A(x^F, x^H$ respectively) is in $\mathcal{F}_{(\omega,\omega_0)}$. Thus, $\pi x = \pi x^A = \pi_0$ which implies that $\pi_A = 0$ (analogously, $\pi_F = \pi_H = 0$).

Case 3: As the incidence vectors x and $\overline{x}$ corresponding to solutions shown in Figures 25(a) and 25(b) are in $\mathcal{F}_{(\omega,\omega_0)}$, we have $\pi x = \pi\overline{x} = \pi_0$, and thus $\pi_G = 0$.

Case 4: Consider the solution illustrated in Figure 26 whose incidence vector belongs to $\mathcal{F}_{(\omega,\omega_0)}$.

If we remove $J(K, L)$ from x we obtain a new feasible solution whose incidence vector $x^J(x^K, x^L$ respectively) is in $\mathcal{F}_{(\omega,\omega_0)}$. Thus, $\pi_J = \pi_{J'} = 0$ ($\pi_K = \pi_{K'} = \pi_L = \pi_{L'} = 0$).

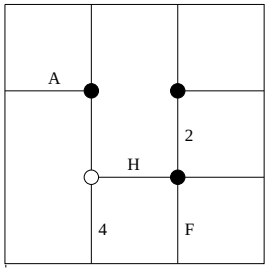

Figure 24: A solution with incidence vector x.

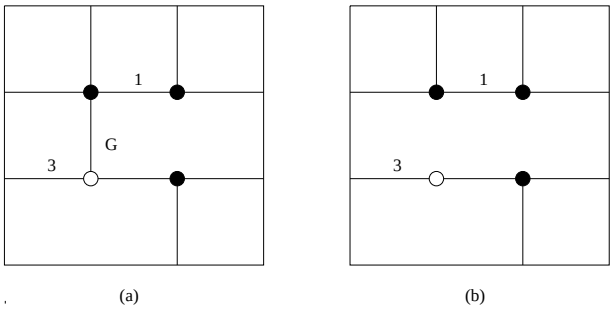

Figure 25: (a) A solution with incidence vector $x = (1, 0, 1, 0, 1, 1, \ldots, 1)$. (b) A solution with incidence vector $\overline{x}$ obtained from x by setting $\overline{x}_G = 0$.

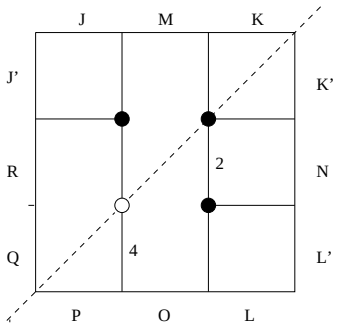

Figure 26: A solution with incidence vector x. The axis of symmetry of the inequality $x_1 + x_2 + x_3 + x_4 \geq 2$ is indicated by the dotted line

If we remove $M(N,O,P)$ from x we obtain a new feasible solution whose incidence vector $x^M(x^N, x^O, x^P$ respectively) is in $\mathcal{F}_{(\omega,\omega_0)}$. Thus, $\pi_M = \pi_N = \pi_O = \pi_P = 0$.

From the solution shown in Figure 27, we conclude $\pi_Q = \pi_R = 0$.

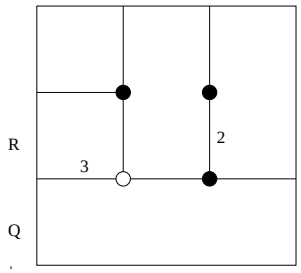

Figure 27: A solution with incidence vector $x = (0,1,1,0,1,1,\ldots,1)$. Let $x^Q(x^R)$ incidence vector obtained from x by removing segment Q (R respectively).

Therefore, from the previous cases, we have that $\pi_1 = \pi_2 = \pi_3 = \pi_4 = \pi_0/2$. Finally, we conclude that there is some $\alpha \in \mathbb{R}_+$ such that:

$$\pi_i = \begin{cases} \alpha & \forall\, i \in \{1,2,3,4\} \\ 2\alpha & for\ \ i = 0 \\ 0 & \forall\, i \in GI(P) \setminus \{1,2,3,4\} \end{cases}$$

□

Proof of Theorem 4.8: Sufficiency: Denote by $\omega x \geq \omega_0$ the inequality $x_1+x_2+x_3+x_4 \geq 1$ and let $\mathcal{F}_{(\omega,\omega_0)} = \{x \in \mathcal{P}_\mathcal{R} \ : \ \omega x = \omega_0\}$ the face defined by it. Notice that $\mathcal{F}_{(\omega,\omega_0)} \neq \mathcal{P}_\mathcal{R}$ since the point $\mathbb{1}_m \in \mathcal{P}_\mathcal{R}$, and $\mathbb{1}_m \notin \mathcal{F}_{(\omega,\omega_0)}$. Assume that $\pi x \geq \pi_0$ is a valid inequality for $\mathcal{P}_\mathcal{R}$ such that $\mathcal{F}_{(\omega,\omega_0)} \subseteq \mathcal{F}_{(\pi,\pi_0)} = \{x \in \mathcal{P}_\mathcal{R} \ : \ \pi x = \pi_0\}$. We have to show that $\pi = \alpha\omega$ and $\pi_0 = \alpha\omega_0$ for some $\alpha \in \mathbb{R}_+$.

By Lemma 4.1, we know that $\pi_i = 0$ for all grid segments i external to the support rectangle of $x_1 + x_2 + x_3 + x_4 \geq 1$.

Case 1: Consider the solution in Figure 28 whose incidence vector belongs to $\mathcal{F}_{(\omega,\omega_0)}$.

As x^A $(x^C, x^E, x^F, x^G, x^H)$ is in $\mathcal{F}_{(\omega,\omega_0)}$, so $\pi_i = 0 \ \ \forall i \in \{A,C,E,F,G,H\}$. Symmetrically, we can show that $\pi_i = 0 \ \ \forall i \in \{A',C',E',F',G',H'\}$.

Case 2: Consider the solution depicted in Figure 29.

Removing the segment J (B) from vector x we obtain incidence vector x^J (x^B). As x and x^J (x^B) are in $\mathcal{F}_{(\omega,\omega_0)}$, we conclude that $\pi_J = 0$ $(\pi_B = 0)$. Again, by symmetry, we can conclude that $\pi_{B'} = \pi_{J'} = 0$.

Case 3: Look at the solutions in Figure 30.

As x and $\overline{x}$ are in $\mathcal{F}_{(\omega,\omega_0)}$ we conclude that $\pi_D = 0$. By symmetry we can show that $\pi_{D'} = 0$.

Case 4: Look at the solution in Figure 31.

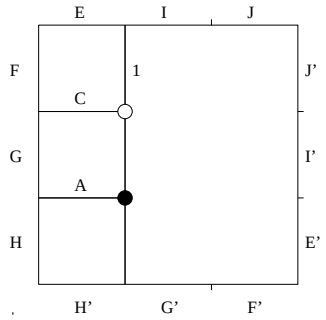

Figure 28: Solution with incidence vector x. Assume x^A (x^C, x^E, x^F, x^G, x^H) the incidence vector obtained from x removing the segment A (C, E, F, G, H respectively).

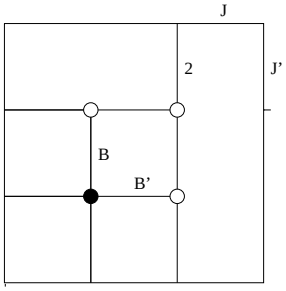

Figure 29: Solution with incidence vector x.

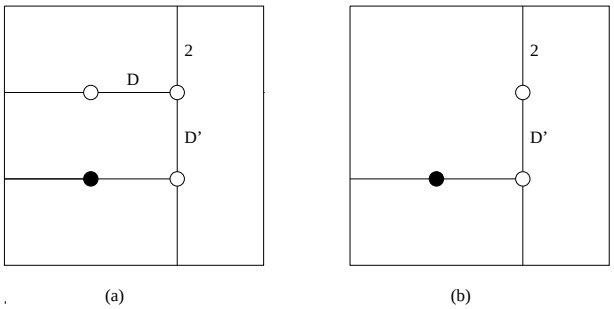

Figure 30: (a) Solution with incidence vector x. (b) Solution with incidence vector $\overline{x}$.

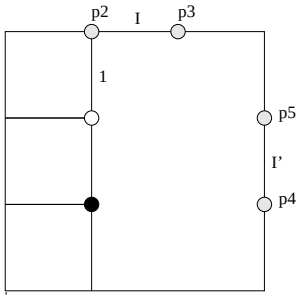

Figure 31: Solution with incidence vector x. The points p_2, p_3, p_4 and p_5 are points at the boundary of the rectangle support of the inequality $x_1 + x_2 + x_3 + x_4 \geq 1$.

Sub-case 4.1: If the point p_3 (p_5) is a Steiner point, then assume $\overline{x}$ the incidence vector obtained from x when we remove the segments incident to p_3 (p_5). As x and $\overline{x}$ are in $\mathcal{F}_{(\omega,\omega_0)}$, we conclude that $\pi_I = 0$ ($\pi_{I'} = 0$).

Sub-case 4.2: If the point p_2 (p_4) is a Steiner point and p_3 (p_5) is a terminal point, then assume x the incidence vector of the solution in Figure 29 and $\overline{x}$ the incidence vector obtained from x when we remove the segments incident to p_2 (p_4). Note that x and $\overline{x}$ are in $\mathcal{F}_{(\omega,\omega_0)}$, so $\pi_I = 0$ ($\pi_{I'} = 0$).

Thus we have $\pi_i = 0 \ \forall i \in GI(P) \setminus \{1,2,3,4\}$ and $\pi_1 = \pi_4 = \pi_0$ (rotating the solution in Figure 28); $\pi_2 = \pi_3 = \pi_0$ (rotating the solution in Figure 29); $\pi_1 = \pi_2 = \pi_0$ (cases 1 e 2), and therefore, $\pi_1 = \pi_2 = \pi_3 = \pi_4 = \pi_0$.

Thus we can conclude that there exists some $\alpha \in \mathbb{R}_+$ such that

$$\pi_i = \begin{cases} \alpha & \forall\, i \in \{1,2,3,4\} \\ \alpha & for\ \ i = 0 \\ 0 & \forall\, i \in GI(P) \setminus \{1,2,3,4\} \end{cases}$$

□

Proof of Theorem 4.9: Denote by $\omega x \geq \omega_0$ the Class V inequality and let $\mathcal{F}_{(\omega,\omega_0)} = \{x \in \mathcal{P}_\mathcal{R} \ : \ \omega x = \omega_0\}$ the face defined by it. Notice that $\mathcal{F}_{(\omega,\omega_0)} \neq \mathcal{P}_\mathcal{R}$ since the point $\mathbb{1}_m \in \mathcal{P}_\mathcal{R}$, and $\mathbb{1}_m \notin \mathcal{F}_{(\omega,\omega_0)}$. Assume that $\pi x \geq \pi_0$ is a valid inequality for $\mathcal{P}_\mathcal{R}$ such that $F\omega \subseteq \mathcal{F}_{(\pi,\pi_0)} = \{x \in \mathcal{P}_\mathcal{R} \ : \ \pi x = \pi_0\}$. We have to show that $\pi = \alpha\omega$ and $\pi_0 = \alpha\omega_0$ for some $\alpha \in \mathbb{R}_+$.

By Lemma 4.1, we know that $\pi_i = 0$ for all grid segments i external to the support rectangle of the Class V inequality.

Case 1: Consider the solution given in Figure 32.

As x and x^A ($x^B, x^C, x^F, x^I, x^M, x^{N'}$) is in $\mathcal{F}_{(\omega,\omega_0)}$, so $\pi_A = \pi_B = \pi_C = \pi_F = \pi_I = \pi_M = \pi_{N'} = 0$. As A and A', B and B', C and C', F and F', I and I', M and M',N and N' are symmetric segments we can show that $\pi_{A'} = \pi_{B'} = \pi_{C'} = \pi_{F'} = \pi_{I'} = \pi_{M'} = \pi_N = 0$.

Case 2: Observe the solution in Figure 33.

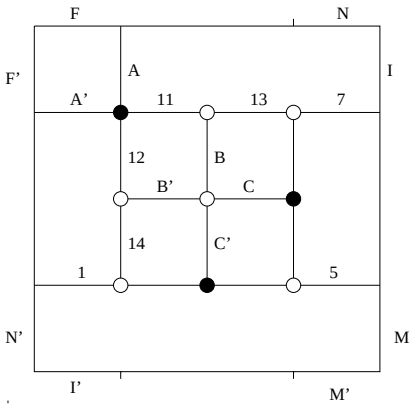

Figure 32: Solution with incidence vector x. Assume x^A ($x^B, x^C, x^F, x^I, x^M, x^{N'}$) be the incidence vector obtained x when we remove the segment A (B, C, F, I, M, N' respectively).

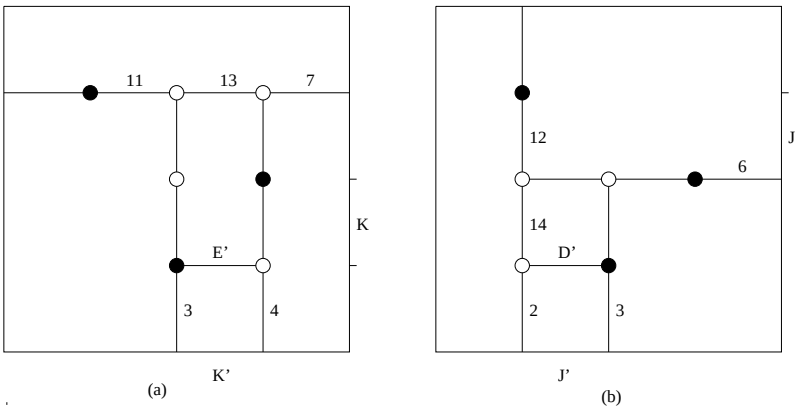

Figure 33: (a) Solution with incidence vector x. Removing the segment $E^{'}$ ($K^{'}$) from x we obtain the incidence vector $x^{E'}$ ($x^{K'}$). (b) Solution with incidence vector $\overline{x}$. Removing the segment D' (J') from $\overline{x}$ we obtain the incidence vector $\overline{x}^{D'}$ ($\overline{x}^{J'}$).

Notice that x and $x^{E'}$ (x and $x^{K'}$) are in $\mathcal{F}_{(\omega,\omega_0)}$ and $\overline{x}$ and $\overline{x}^{D'}$ ($\overline{x}$ and $\overline{x}^{J'}$) are in $\mathcal{F}_{(\omega,\omega_0)}$. So $\pi_{D'} = \pi_{E'} = \pi_{J'} = \pi_{K'} = 0$. As D and D', E and E', J and J', K and K' are symmetric segments we can proof that $\pi_D = \pi_E = \pi_J = \pi_K = 0$.

Case 3: Observe the solution in Figure 34.

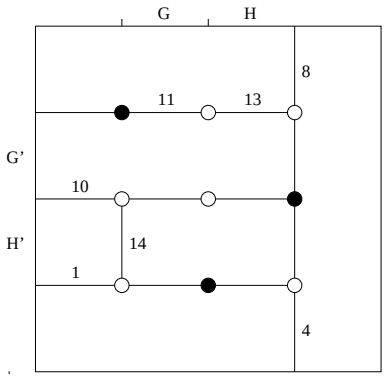

Figure 34: Solution with incidence vector x. Removing the segment G' (H') from x we obtain the incidence vector $x^{G'}$ ($x^{H'}$).

As x and $x^{G'}$ (x and $x^{H'}$) are in $\mathcal{F}_{(\omega,\omega_0)}$, so $\pi_{G'} = \pi_{H'} = 0$. As G and G', H and H' are symmetric segments, so $\pi_G = \pi_H = 0$.

The following results can be derived: $\pi_i = 0\ \forall i \in GI(P) \setminus \{1,\ldots,14\}$; $\pi_1 = \pi_2$, $\pi_4 = \pi_5$ and $\pi_7 = \pi_8$ (this can be seen by replacing the corresponding pair of segments in Figure 32); $\pi_1 = \pi_2 = \pi_3$ (solutions in Figures 33(a) and 35(a)), $\pi_4 = \pi_6$ (solutions in Figures 33(a) and 35(b)), $\pi_6 = \pi_8$ (solution in Figure 36); $\pi_{11} + \pi_{13} = \pi_{12} + \pi_{14} = 0$ (solutions in Figures 36(a) e 37(a)); $\pi_2 = \pi_4$ ($\pi_6 = \pi_7 = \pi_8$ and solutions in Figures 33); $\pi_i = \frac{1}{3}\pi_0\ \ i = 1,\ldots,8$ (previous relations and solution in Figure 32); $\pi_{10} + \pi_{12} = \frac{1}{3}\pi_0$ ($\pi_3 = \pi_6 = \frac{1}{3}\pi_0$ and solution in Figure 37(b)); $\pi_9 + \pi_{11} = \frac{1}{3}\pi_0$ (symmetric situation to $\pi_{10} + \pi_{12} = \frac{1}{3}\pi_0$); $\pi_{10} + \pi_{14} = 0$ ($\pi_2 = \pi_4 = \pi_8 = \frac{1}{3}\pi_0$, $\pi_{11} + \pi_{13} = 0$ and solution in Figure 37(c)); $\pi_9 + \pi_{13} = 0$ (symmetric to $\pi_{10} + \pi_{14} = 0$); $\pi_{10} = \pi_{12} = -\pi_{14}$ (from $\pi_{12} + \pi_{14} = 0$ and $\pi_{10} + \pi_{14} = 0$); $\pi_9 = \pi_{11} = -\pi_{13}$ (symmetric to $\pi_{10} = \pi_{12} = -\pi_{14}$); $\pi_{10} = \pi_{12} = \frac{1}{6}\pi_0$ and $\pi_{14} = -\frac{1}{6}\pi_0$ (from $\pi_{10} = \pi_{12} = -\pi_{14}$ and $\pi_{10} + \pi_{12} = \frac{1}{3}\pi_0$); $\pi_9 = \pi_{11} = \frac{1}{6}\pi_0$ and $\pi_{13} = -\frac{1}{6}\pi_0$ (similar to previous relation).

So we can conclude that there exists some $\alpha \in \mathbb{R}_+$ such that

$$\pi_i = \begin{cases} \alpha & \forall\, i \in \{1,2,\ldots,8\} \\ \alpha/2 & \forall\, i \in \{9,\ldots,12\} \\ -\alpha/2 & \forall\, i \in \{13,14\} \\ 3\alpha & for\ \ i = 0 \\ 0 & \forall\, i \in GI(P) \setminus \{1,\ldots,14\} \end{cases}$$

□

Proof of Theorem 4.10: Denote by $\omega x \geq \omega_0$ the Class VI inequality and let $\mathcal{F}_{(\omega,\omega_0)} = \{x \in \mathcal{P}_{\mathcal{R}} : \omega x = \omega_0\}$ the face defined by it. Notice that $\mathcal{F}_{(\omega,\omega_0)} \neq \mathcal{P}_{\mathcal{R}}$ since the point

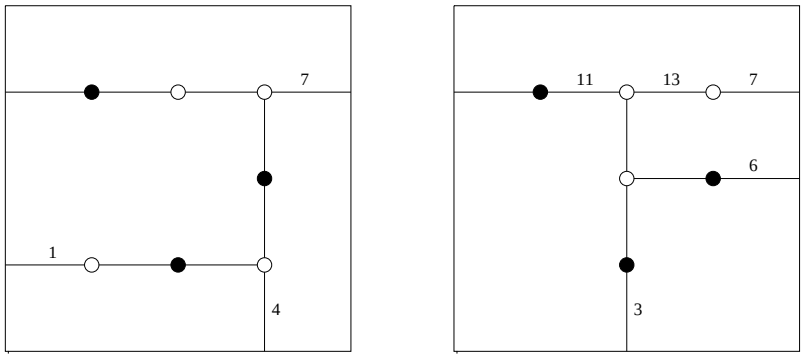

(a) (b)

Figure 35: (a) and (b) Solutions with incidence vectors x and $\overline{x}$.

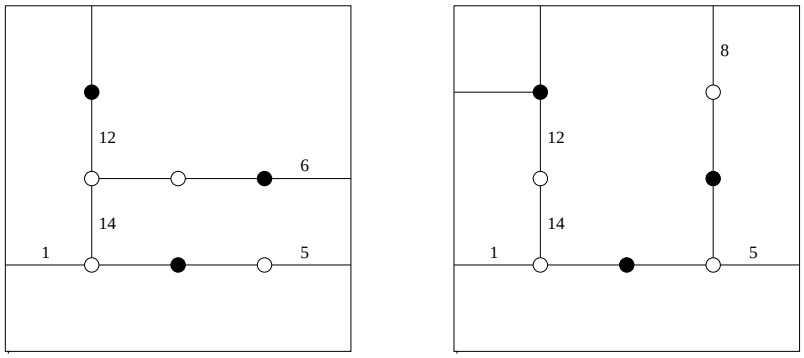

(a) (b)

Figure 36: (a) and (b) Solutions with incidence vectors x and $\overline{x}$.

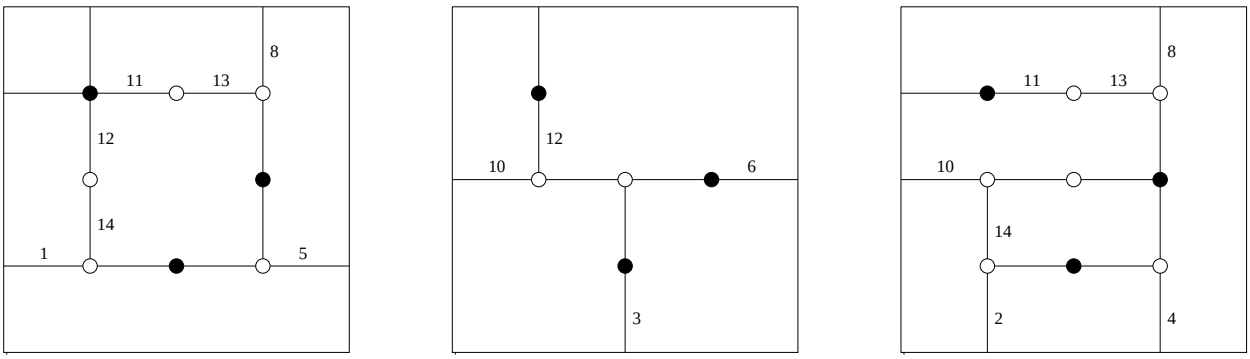

(a) (b) (c)

Figure 37: (a), (b) and (c) Solutions with incidence vectors x, $\overline{x}$ and x^*.

$\mathbb{1}_m \in \mathcal{P}_{\mathcal{R}}$, and $\mathbb{1}_m \notin \mathcal{F}_{(\omega,\omega_0)}$. Assume that $\pi x \geq \pi_0$ is a valid inequality for $\mathcal{P}_{\mathcal{R}}$ such that $\mathcal{F}_{(\omega,\omega_0)} \subseteq \mathcal{F}_{(\pi,\pi_0)} = \{x \in \mathcal{P}_{\mathcal{R}} \ : \ \pi x = \pi_0\}$. We wish to show that $\pi = \alpha\omega$ and $\pi_0 = \alpha\omega_0$ for some $\alpha \in \mathbb{R}_+$.

By Lemma 4.1, we know that $\pi_i = 0$ for all grid segments i external to the support rectangle of the Class VI inequality.

Case 1: Consider the solution shown in Figure 38.

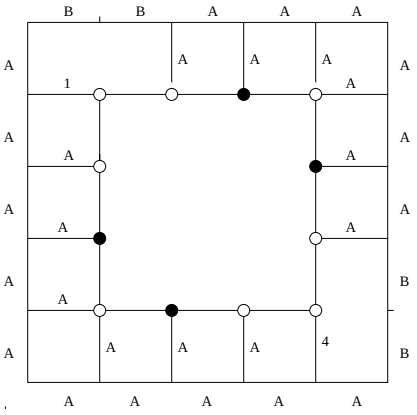

Figure 38: Solution with incidence vector x. Let x^A be the incidence vector obtained from x when we remove some segment A.

Notice that x and x^A are in $\mathcal{F}_{(\omega,\omega_0)}$, so $\pi_A = 0$. Considering the symmetric solution of the solution given in Figure 38, where we make $x_2 = x_3 = 1$ instead $x_1 = x_4 = 1$, we obtain $\pi_B = 0$.

Case 2: Consider the solution shown in Figure 39.

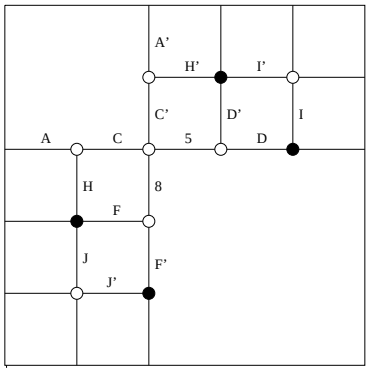

Figure 39: Solution with incidence vector x. Removing some segment labeled with a letter, except the segments A, A', C, C', D, F', we obtain a solution with incidence vector $\overline{x}$. Now if we remove the set of segments A, C, H or A', C', H' from x we obtain a solution with incidence vector $\overline{x}^*$.

Notice that x and $\overline{x}$ are in $\mathcal{F}_{(\omega,\omega_0)}$ and x and $\overline{x}^*$ are in $\mathcal{F}_{(\omega,\omega_0)}$. Thus $\pi_i = 0$ for all $i \in \{C, C', D', F, H, H', J, J', I, I'\}$. As the segments D and D', F and F' are symmetric, so $\pi_D = \pi_{F'} = 0$.

Case 3: Consider the solution shown in Figure 40.

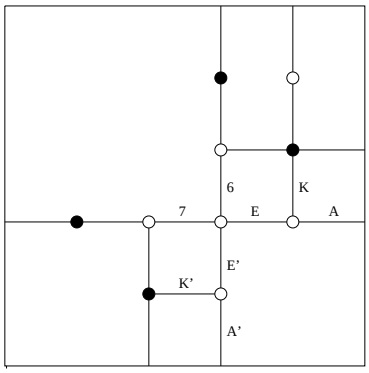

Figure 40: Solution with incidence vector x. Removing from x the segment K (K') we obtain the incidence vector $\overline{x}^K$ ($\overline{x}^{K'}$), or if we remove the set of segments A, E, K (A', E', K') we obtain the vector $\overline{x}^*$.

As x and $\overline{x}$ are in $\mathcal{F}_{(\omega,\omega_0)}$ and x and $\overline{x}^*$ are in $\mathcal{F}_{(\omega,\omega_0)}$, we conclude that $\pi_E = \pi_{E'} = \pi_K = \pi_{K'} = 0$.

Case 4: Observe the solutions in Figure 41.

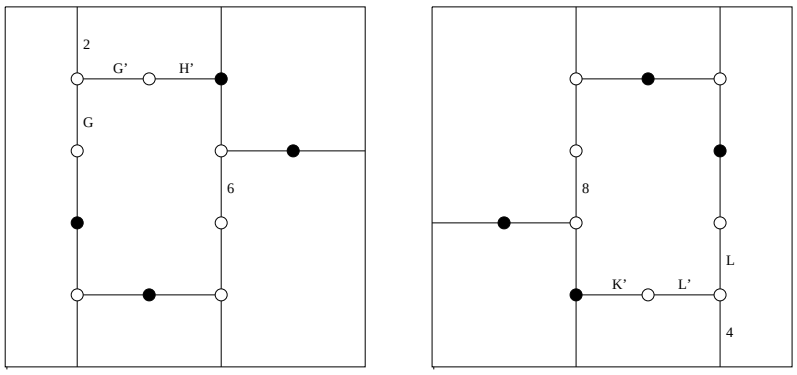

Figure 41: (a) Solution with incidence vector x. Removing the segments G' and H' from x we obtain a solution with incidence vector x^*. (b) Solution with incidence vector $\overline{x}$. Removing the segments K' and L' from $\overline{x}$ we obtain a solution with incidence vector $\overline{x}^*$.

Notice that x and x^* are in $\mathcal{F}_{(\omega,\omega_0)}$ and $\overline{x}$ and $\overline{x}^*$ are in $\mathcal{F}_{(\omega,\omega_0)}$, so $\pi_{G'} = \pi_{L'} = 0$. As G and G', L and L' are symmetric, we conclude that $\pi_G = \pi_L = 0$.

In summary, we have that: $\pi_1 = \pi_2$ and $\pi_3 = \pi_4$ (case 1); $\pi_1 + \pi_3 = \pi_5 + \pi_8 = \pi_6 + \pi_7 = \pi_2 + \pi_6 = \pi_0$ (cases 1, 2, 3 and 4), and therefore, $\pi_1 = \pi_2 = \pi_7$; $\pi_1 + \pi_7 = \pi_0$, and therefore, $\pi_1 = \pi_2 = \pi_6 = \pi_7 = \pi_0/2$ (Figure 42(a)); $\pi_1 = \pi_5$ (case 1 and Figure 42(b)); $\pi_3 = \pi_4 = \pi_8$ (case 2 and Figure 42(b)); $\pi_3 = \pi_4 = \pi_5 = \pi_8$ (case 2 and Figure 42(b)); $\pi_1 = \pi_8$ (cases 1, 2 and relation $\pi_4 = \pi_5$), and therefore, $\pi_i = \pi_0/2 \ \forall i \in \{1, \ldots, 8\}$ and $\pi_i = 0 \ \forall i \in GI(P) \setminus \{1, \ldots, 8\}$.

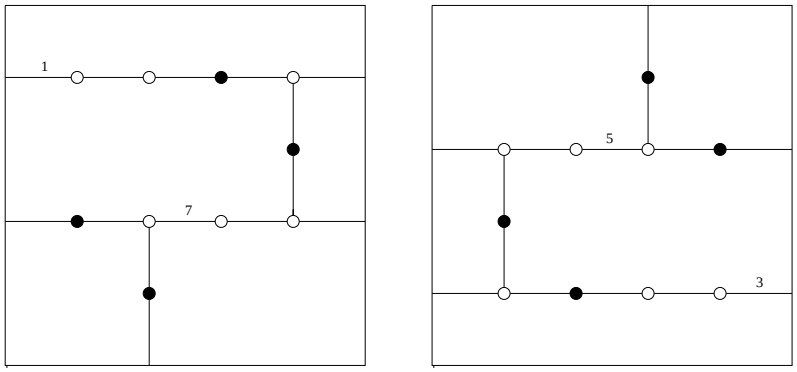

Figure 42: (a) and (b) Solutions with incidence vectors x and $\overline{x}$.

Thus we can conclude that there exists some $\alpha \in \mathbb{R}_+$ such that

$$\pi_i = \begin{cases} \alpha & \forall\, i \in \{1, \ldots, 8\} \\ 2\alpha & for\ \ i = 0 \\ 0 & \forall\, i \in GI(P) \setminus \{1, \ldots, 8\} \end{cases}$$

□

References

[1] CPLEX Optimization, Inc. Using the CPLEX Callable Library. Manual, 1994.

[2] D. Z Du, L. Q. Pan, and M. T. Shing. Minimum Edge Length Guillotine Rectangular Partition. Technical report, Mathematical Sciences Research Institute, University of California, Jan. 1986.

[3] T. F. Gonzalez, M. Razzazi, M. T. Shing, and S. Q. Zheng. On Optimal Guillotine Partitions Approximating Optimal d-Box Partitions. *Computational Geometry*, 4:1–11, 1994.

[4] T. F. Gonzalez, M. Razzazi, and S. Q. Zheng. An Efficient Divide-and-Conquer Approximation Algorithm for Partitioning into d-boxes. *International Journal of Computational Geometry and Applications*, 3(4):281–287, 1993.

[5] T. F. Gonzalez and S. Q. Zheng. Bounds for Partitioning Rectilinear Polygons. *Proc. Symp. Computacional Geometry*, pages 281–287, June 1985.

[6] T. F. Gonzalez and S. Q. Zheng. Improved Bounds for Rectangular and Guillotine Partitions. *J. Symbolic Computation*, 7:591–610, 1989.

[7] T. F. Gonzalez and S. Q. Zheng. Approximation Algorithms for Partitioning a Rectangle with Interior Points. *Algorithmica*, 5:11–42, 1990.

[8] K. L. Hoffman and M. W. Padberg. Solving Airline Crew Scheduling Problems by Branch-and-Cut. *Mangement Science.*, 39(6):657–682, 1993.

[9] M. Jünger, G. Reinelt, and S. Thienel. Practical Problem Solving with Cutting Plane Algorithms in Combinatorial Optimization. Technical report, Institut für Informatik, Universität zu Köln, 1994.

[10] C. Levcopoulos. Fast Heuristics for Minimum Length Rectangular Partitions of Polygons. *Proceedings of the 2nd Computational Geometry Conference*, June 1986.

[11] A. Lingas, R.Y. Pinter, R.L. Rivest, and A. Shamir. Minimum Edge Length Partitioning of Rectlinear Polygons. In *Proceedings of the 20th Annual Allerton Conference Communication, Control, and Computing*. University of Illinois, 1982.

[12] G. L. Nemhauser and L. A. Wolsey. *Integer and Combinatorial Optimization.* John Wiley & Sons, 1988.

[13] D. M. Ryan and B. A. Foster. An Integer Programming Approach to Scheduling. *A. Wren (ed.) Computer Scheduling of Public Transport Urban Passenger Vehicle and Crew Scheduling, North-Holland, Amsterdam*, pages 269–280, 1981.

[14] M. W. P. Savelsbergh and G. L. Nemhauser. Functional Description of MINTO, a Mixed INTeger Optimizer. Manual version 2.3, 1996.